

FINAL TECHNICAL REPORT
Award Number: G14AP00099

Title: “Updating Liquefaction Probability Curves, Seismic Hazard Model, and Urban Seismic Hazard Maps with Public Outreach for Memphis and Shelby County, Tennessee”

Chris H. Cramer, PI and Gary Patterson, Co-PI
Center for Earthquake Research and Information
University of Memphis
3890 Central Ave
Memphis, TN 38152-3050
901-678-4992
FAX: 901-678-4734
cramer@ceri.memphis.edu
glpttrsn@memphis.edu

David Arellano, Co-PI
Department of Civil Engineering, University of Memphis
104 Engineering Science Bldg.
Memphis, TN 38152-3050
901-678-3272; FAX: 901-678-3026
darellan@memphis.edu

August 1, 2014 – July 31, 2015

Submitted: October 30, 2015

“Research supported by the U.S. Geological Survey (USGS), Department of Interior, under USGS award numbers G14AP00099. The views and conclusions contained in this document are those of the authors and should not be interpreted as necessarily representing the official policies, either expressed or implied, of the U.S. Government.”

Abstract

In 2012-2013, Memphis urban seismic hazard maps were updated and expanded to all of Shelby County from the original six 7.5' quadrangles in 2004 [U.S. Geological Survey (USGS) grant G12AP20079]. The 2013 revised Memphis urban seismic hazard maps used an updated 3D geologic model, which increased hazard significantly. In 2014-2015 we revised the geotechnical aspects of the 2004 hazard maps that could not be addressed in the 2012-2013 update and adopted the USGS National Seismic Hazard Mapping Project (NSHMP) 2014 hazard model. We generated revised probabilistic and scenario ground-motion and liquefaction urban hazard maps for 12+ quadrangles covering Shelby Co. The resulting 2015 probabilistic Memphis urban hazard maps showed similar seismic hazard (within 10%) to the 2013 maps, but reduced seismic hazard for the scenario maps compared to the 2013 maps due to decrease ground motion predictions by the 2014 NSHMP attenuation relations and weights. Liquefaction hazard changes are mainly in the predictions for loess and alluvium, which show reductions and increases, respectively, from the 2004 equivalent hazard maps due to improved modeling of liquefaction response from our 2014-2015 study.

A public and professional outreach workshop was held July 28, 2015 to raise public, business, and professional awareness of Memphis area earthquake hazards, and to disseminate the revised urban hazard maps produced in 2015. The one-day workshop focused on (1) explaining the hazard posed to Memphis by the New Madrid seismic zone and other nearby seismic sources in the 2014 NSHMP model, (2) dissemination of the updated Memphis urban hazard maps, (3) interaction with the professional, business, and public-sector user community concerning their needs, and (4) continuing hazard mapping and mitigation efforts for Memphis and west Tennessee.

Introduction

The 2012-2013 Memphis geologic model significantly increased the seismic hazard in the Memphis area (Cramer et al., 2014). Stevens (2007) and the 2012 geologic data updated and expanded the areal coverage of the upper 100 m and the Csontos (2007) Mississippi embayment model expanded the areal coverage of the deeper sediment section of the 3D geologic model for Shelby Co. Included in the 2012-2013 geologic model improvements is a better modeling of sharp changes in layer thickness due to faults and/or erosional truncation of strata that affects seismic hazard. For the first Memphis urban seismic hazard maps, Gomberg et al. (2003) fit smoothed surfaces through these sharper changes and failed to properly sample the Mississippi River floodplain geology. Additionally, the USGS National Seismic Hazard Mapping Project (NSHMP) updated their 2008 national seismic hazard model (use in the 2012-2013 study) to the 2014 model (use in this study). For the Memphis and New Madrid seismic zone region, the 2014 NSHMP hazard model includes additional ground motion prediction equations that could lower hazard significantly and additional seismic sources in the region that can raise hazard. This would impact the 2013 Memphis urban hazard maps and the 2014 NSHMP updates have been applied to dampen the large changes in hazard from the 2004 maps.

As part of this grant, we held a workshop to disseminate these new Memphis urban seismic and liquefaction hazard maps and to gain input from the technical and user communities in the Memphis area. The first part of this report discusses the updating of the Memphis urban hazard maps and its results. The second part discusses the workshop and its products.

Updating the Memphis Urban Hazard Maps

Methodology

Earthquake ground motions at any location basically depend on the size of the earthquake (magnitude), how ground motions decay with distance from the earthquake faulting (attenuation with distance), and how soils beneath a site increase or decrease amplitudes at certain frequencies in the ground motion (site amplification based on local geology). Earthquake hazard basically depends on the rate at which earthquakes occur in the region surrounding a site (recurrence) and the magnitudes of those earthquakes. Larger earthquakes have bigger associated ground motions over a wider area and hence can cause more damage and pose a greater hazard than smaller earthquakes. Thus, earthquake hazard is mainly determined by the rate of large earthquakes (magnitude 7's in the central and eastern US). For the New Madrid seismic zone, dated paleoliquefaction features indicate that $M > 7.0$ earthquakes occur on average every 500 years (Kelson et al., 1996; Tuttle et al., 2002), and recently published geodetic observations confirm continued strain accumulation and the potential for future activity (Frankel et al., 2012), which poses a significant hazard in the Memphis area and the central U.S.

Probabilistic seismic hazard estimates answer the question "What is the likelihood of a given level of ground shaking being exceeded at a site?" This involves knowing where the earthquakes occur in the region (the distance to each earthquake source from the site), the relationship between earthquake magnitude and frequency of occurrence for each earthquake source region (magnitude-frequency distribution), and how big the ground motion is for every earthquake magnitude and distance from the site (ground motion attenuation relation). The national seismic

hazard maps combine the probabilities from these distributions for each earthquake source in the region, but does so for a uniform soil condition (site amplification). That is, the national maps do not take into account the effects of local near-surface geology on earthquake ground motions.

Scenario seismic hazard estimates answer the question “Given that a specific scenario earthquake occurs, what level of ground shaking can be expected to happen at a site?” Unlike probabilistic seismic hazard estimates, only one scenario earthquake rupture is considered, usually one that significantly impacts the site or region being considered. Scenario maps may be calculated for a uniform soil condition that generally occurs in the area being considered, or they can take into account the effects of the variation of local geology on the earthquake ground motions.

Urban seismic hazard maps add in the effect of local geology on the amplification of earthquake ground motions in order to have more realistic ground motions for earthquake hazard analysis within the study area. To do this, information is needed about the local distribution and thicknesses of soil in the urban area. Basically, two pieces of information are needed: what are the thicknesses of each soil type at a site (lithology) and what are each soil type’s physical (geotechnical) properties that affect ground motion amplification. Site amplification is determined by taking a soil profile (soil type thicknesses and physical properties) and subjecting that soil profile to earthquake shaking (time history) originating in the solid rock at the bottom of the soil profile to calculate the expected shaking at the ground surface. The change in amplitude of the shaking at a given frequency from the bottom to the top of the soil profile is site amplification.

Nonlinear soil behavior at strong ground motions (> 0.1 g) significantly affects observed ground motions, particularly at short periods (< 1.0 s). Because Memphis is within 50 km of the New Madrid seismic zone, the nonlinear soil effects are important. As demonstrated by the original Memphis urban hazard maps, short period ground motions (peak ground acceleration [PGA] and 0.2 s spectral acceleration [Sa]) are significantly reduced and ground motion gradients across Shelby Co. reduced relative to the national hazard maps, which are without local soil effects (Cramer et al., 2004, 2006). At long periods (1.0 s and greater), nonlinearity is not significant and hence the thick soils beneath Memphis strongly amplify long period ground motions. Changes in the 2008 and 2014 USGS national seismic hazard models tend to reduce ground motions relative to the 2002 model, however soil nonlinearity at short periods will tend to counter this trend because decreased ground motions will decrease nonlinear effects, which will increase relative soil amplification. Strong shallow soil resonances can counter the nonlinear effects on ground motions, as found in the 2012-2013 geology model update: 10 m and less of low-velocity (< 250 m/s) alluvium/loess had minimal effects, 10 to 30 m of alluvium/loess had strong resonance and increased hazard, and greater than 30 m of alluvium/loess had strong nonlinearity and decreased hazard (Cramer et al., 2014).

Liquefaction hazard maps are generated from liquefaction hazard curves. These curves combine seismic peak ground acceleration (PGA) hazard curves that include the effects of site geology and liquefaction probability curves that represent the susceptibility of a site’s shallow soil to liquefaction due to earthquake magnitude and PGA at the site. A seismic hazard curve just represents the probability of exceeding a given level of ground motion at a site and is the basic result of a probabilistic seismic hazard analysis. Seismic hazard curves are used to generate seismic hazard maps. In geotechnical analysis for susceptibility to liquefaction, earthquake magnitude is a proxy for duration of shaking. Geotechnical information needed for liquefaction

susceptibility analysis is lithology (sand or clay), soil type distribution with depth, degree of saturation, density (porosity), and the diffusivity of pore pressure within each lithology. These liquefaction geotechnical properties are often inferred from penetration blow counts from a standard penetration test (SPT) or measured from cone penetrometer tests (CPT). To generate a liquefaction hazard map based on surface geology, a surface geologic map is used in a geographic information system (GIS) to select from a suite of liquefaction hazard maps for each surface soil type generated from that soil type's hazard curves for the region.

Figures 1 and 2 provide a generalized picture of how all the earth science and geological/geotechnical information comes together to generate urban seismic ground motion and liquefaction hazard maps. A lot of disparate information needs to be determined and brought together from a variety of disciplines and sources. Validation and quality control of the information developed must occur for the urban hazard maps to be realistic and beneficial. The information and procedures must reflect our current understanding and the best available science to be credible so that the resulting products can be used with confidence. The ongoing Memphis Technical Working Group (TWG) reviewed the application of the procedures and resulting maps as part of our quality control effort.

How Urban Hazard Maps Are Made - Ground Motion

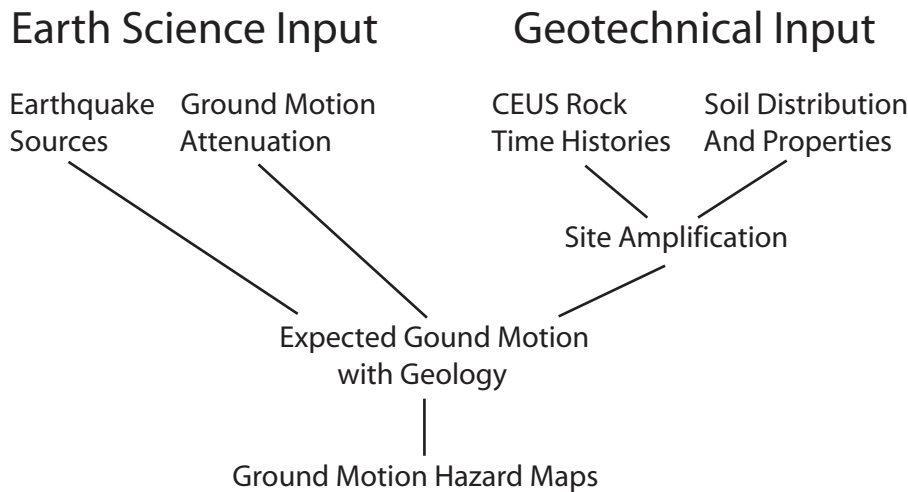


Figure 1.

How Urban Hazard Maps Are Made - Liquefaction

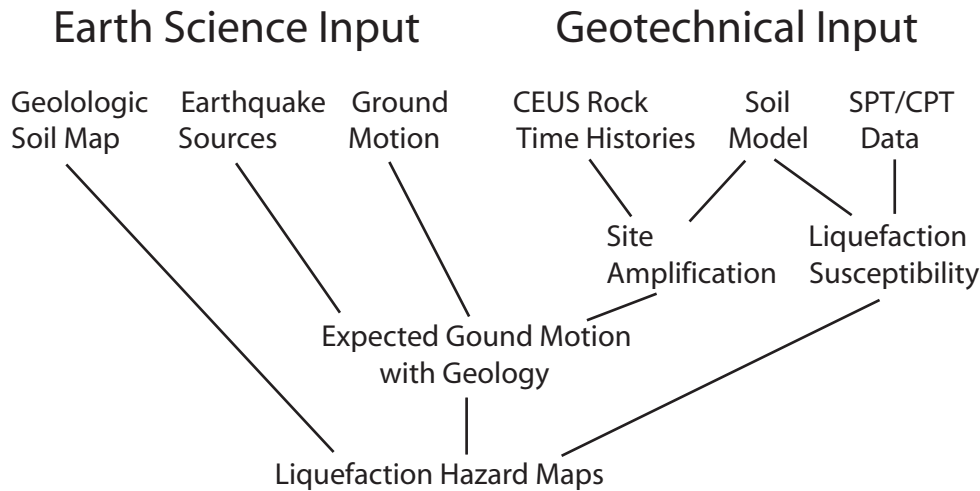


Figure 2.

Originally, Memphis urban seismic hazard maps were generated by applying site amplification distributions inside the hazard integral to modify the hard-rock ground motion prediction equations used in the analysis to site-specific equations for the soil profile under the site or grid point (Cramer, 2003, 2005). When the soil profile is modified, the entire hazard analysis must be redone. For a given site, the probability, $P(A > A_o)$, of exceeding a specific ground motion A_o (Reiter, 1990, equation 10.2) is given by the seismic hazard integral

$$P(A > A_o) = \sum_i \alpha_i \int_M \int_R f_i(M) f_i(R) P(A > A_o | M, R) dR dM, \quad (1)$$

where A is a ground-motion parameter (i.e., PGA or S_a), A_o is the ground motion level to be exceeded, α_i is the annual rate of occurrence of the i^{th} source, M is magnitude, R is distance, $|$ is a conditional probability symbol that means given the variables that follow it, $f_i(M)$ is the probability density distribution of earthquake magnitude of the i^{th} source, and $f_i(R)$ is the probability density distribution of distance from the i^{th} source. Currently, hazard at a site (grid point) is calculated by applying the appropriate site amplification distribution $P(A_s | A_r)$ to the ground-motion attenuation relations within the hazard integral so as to alter them to site-specific attenuation relations (Cramer, 2003, 2005). Thus, in equation 1, $A = A_s$ and $P(A > A_o | M, R)$ becomes $P(A_s > A_o | M, R)$ for a soil site, and

$$P(A_s > A_o | M, R) = 1 - \int_{A_r} P(A_s \leq A_o | A_r) P(A_r | M, R), \quad (2)$$

where

$$P(A_s \leq A_o | A_r) = \int_{A_s: \rightarrow A_o} P(A_s = A_o | A_r) dA \quad (3)$$

and

$$P(A_r | M, R) = d[1 - P(A > A_r | M, R)] / dA. \quad (4)$$

Basically the site amplification distribution alters the rock hazard curve to a soil hazard curve for each earthquake in the hazard model before they are summed into the final soil hazard curve.

For the St. Louis Area Earthquake Hazards Mapping Project and the 2013 Memphis updated urban maps, an alternative approach to site-specific probabilistic seismic hazard calculation has been implemented (Cramer, 2011). The alternative methodology applies the site amplification distribution outside the hazard integral to modify the hard-rock hazard curve (no soil amplification) to a site-specific hazard curve (with soil amplification) for the site or grid point, which saves recalculating the hazard every time the soil profile is updated and improved (factor of 5 or more computational efficiency). Lee (2000) has shown that instead of modifying the hazard curve of each earthquake in the hazard model and summing the resulting site-specific hazard curves to obtain the total site-specific hazard curve, the total hazard curve from the hard-rock hazard calculation can be modified directly by the site amplification distribution to make it site-specific:

$$P(A_s > A_o) = 1 - \int_{A_r} P(A_s \leq A_o | A_r) P(A_r), \quad (5)$$

where $P(A_s \leq A_o | A_r)$ is given by equation 3, and $P(A_r)$ is from the total hard rock hazard curve and is given by

$$P(A_r) = d[1 - P(A_r > A)] / dA. \quad (6)$$

This can be done because the site amplification distribution is explicitly independent of earthquake magnitude and distance and thus can be pulled outside of the seismic hazard integral (equation 1). It may seem that nonlinearity in soil response is implicitly dependent on magnitude and distance, but engineering models of nonlinear response are only dependent on the input level of ground motion at a site. Further, the nature of the total hazard curve at a site emphasizes that the strong ground motions come from the nearest, largest earthquakes and hence nonlinear soil behavior is a function of ground-shaking strength. Comparisons (Figure 3) between these two approaches at the Savannah River Site and for St. Louis indicate that both approaches yield essentially the same hazard result (Lee, 2006, personal communication; Cramer, 2011).

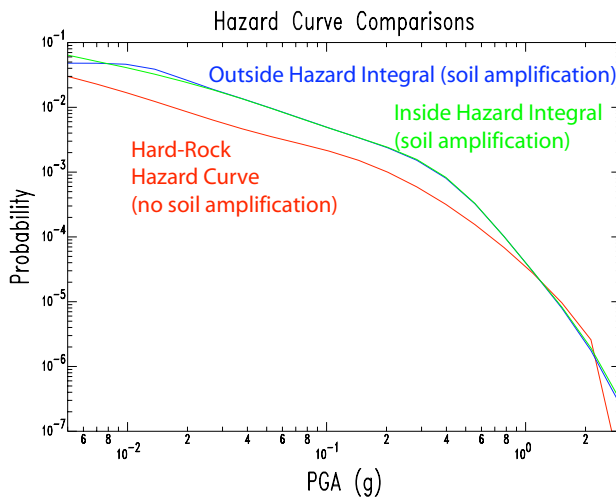


Figure 3: Comparison of hazard curves at a site in the St. Louis area showing the hard-rock total hazard curve (red) without soil amplification and the resulting hazard curves with the effect of site geology using the inside the hazard integral approach (green – Cramer, 2003, 2005) and outside the hazard integral approach (blue – Cramer, 2011).

The alternative methodology assumes that the site amplification distribution is independent of magnitude and distance, which is the case for the Memphis area because the M7 earthquakes expected on the New Madrid seismic zone dominate the seismic hazard and because the site amplification distributions are calculated using an input ground motion at the bottom of the soil profile that is independent of distance from the source (Cramer, 2009). Figure 3 compares the results at the same site for both the inside and outside the hazard integral approaches and shows that the site-specific hazard curves are essentially identical. Thus, for updated Memphis urban seismic hazard maps, the outside the hazard integral methodology was employed in calculating updated urban seismic hazard curves and maps for Memphis.

For the liquefaction hazard maps, the approach of Cramer et al. (2008) used to produce the Memphis liquefaction hazard maps have been applied to all of Shelby Co. Liquefaction potential curves, which are a function of peak ground acceleration (PGA) and earthquake magnitude, have been combined with individual earthquake seismic hazard curves inside the hazard integral to produce liquefaction hazard curves from which liquefaction hazard maps will be produced. The liquefaction hazard integral (Cramer et al., 2008) is given by

$$P(P_{LPI > n} > P_o) = \sum_i \alpha_i \int_M \int_R f_i(M) f_i(R) P(P_{LPI > n} > P_o | A > A_o, M) P(A > A_o | M, R) dR dM, \quad (7)$$

where P_o is a probability that $P_{LPI > n}$ will be exceeded from the liquefaction potential distribution, α_i is the annual rate of occurrence of the i th source, M is magnitude, R is distance, $f_i(M)$ is the probability distribution of earthquake magnitude of the i th source, $f_i(R)$ is the probability distribution of distance from the i th source, $|$ is a conditional probability symbol that means given the variables that follow it, A_o is the liquefaction potential curve value of PGA for an event of magnitude M at P_o , $P(P_{LPI > n} > P_o | A > A_o, M)$ is the liquefaction potential cumulative probability relation or curve, and $P(A > A_o | M, R)$ is the ground motion conditional probability (attenuation relation).

To generate probabilistic liquefaction hazard maps for severe, moderate, and little to no liquefaction hazard ($LPI > 15$, >5 , and <5 , respectively), liquefaction probability curves are needed, which can be generated from a suite of liquefaction potential index calculations for a range of magnitudes and PGAs. A major geotechnical engineering research effort of this study was to generate these liquefaction probability curves for each appropriate surficial geology type on the MAEHMP surface geology maps using the approach of Rix and Romero-Hudock (2006) and the available Memphis CPT and SPT measurements.

Geotechnical Analyses: Updating Liquefaction Probability Curves

A summary of the geotechnical engineering analysis performed to develop updated liquefaction probability curves for each appropriate surficial geology type on the MAEHMP surface geology maps is presented in this section. Background information on the selection of subsurface boring and groundwater level data is initially presented followed by a summary of the procedure used to generate liquefaction probability curves for each appropriate surficial geology type. A comparison summary of the updated liquefaction probability curves compared to the 2005 curves from Rix and Romero-Hudock (2006) is also provided.

Geotechnical Boring Data

Rix and Romero-Hudock (2006) used the Ng et al. (1989) and Hwang et al. (1999) subsurface and Standard Penetration Test (SPT) databases to develop the 2005 liquefaction hazard maps. Ng et al. (1989) gathered 8,500 boring logs from various locations within Shelby County. They divided Shelby County into 30 sec x 30 sec (approximately 762 m (2,500ft.) E-W x 914 m (3,000 ft.) N-S) area grids and mapped the boring locations based on the grids as shown in Figure 4. Ng et al. (1989) consolidated all the data from boring logs within a grid into a single soil profile, termed as interpreted soil profile herein. For example, if a grid contained six boring logs, then soil stratigraphy depths, unified soil classification system (USCS) designations, groundwater depths, Standard Penetration Test (SPT) -*N* values, and any other soil properties included in the logs were averaged and an average interpreted soil profile was developed to represent the subsurface conditions within the grid. This averaging methodology resulted in a total of 623 interpreted soil profiles from the original 8,500 boring logs.

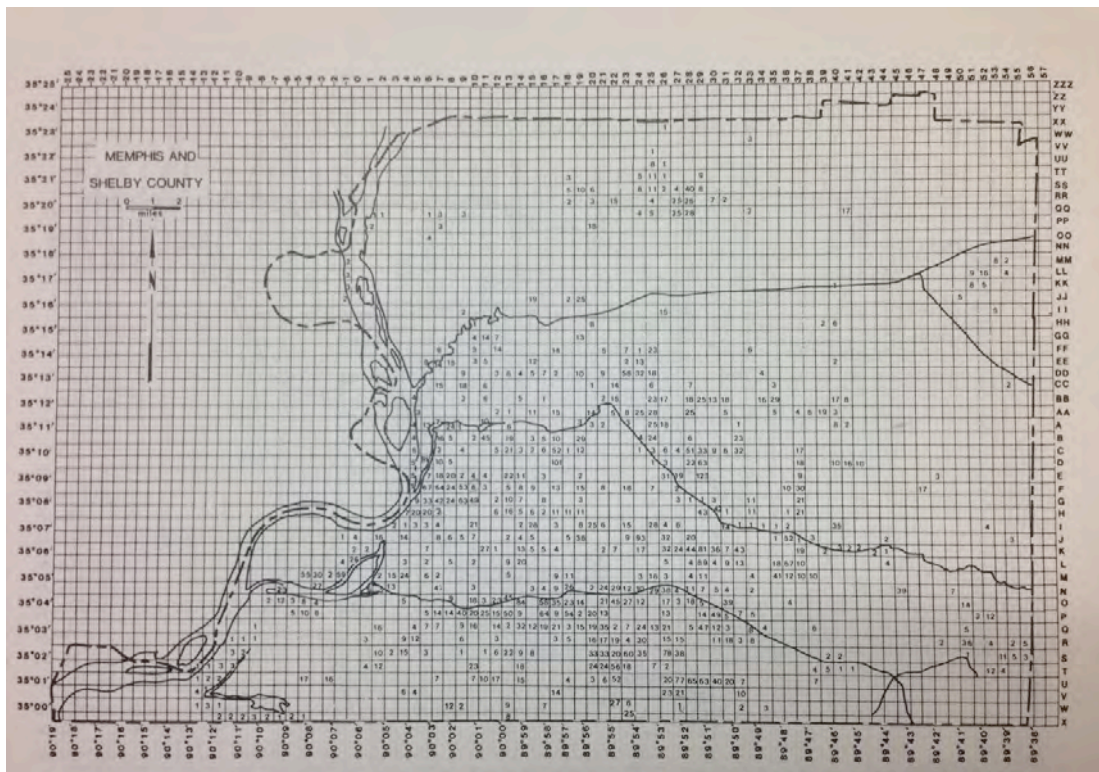


Figure 4. Boring Data Distribution Map (Ng et al., 1989). Number inside each grid is number of soil borings within that grid.

Hwang et al. (1999) used the Ng et al. (1989) 623 interpreted soil profiles and an additional 894 boring logs to prepare a Liquefaction Susceptibility Map of Memphis and Shelby county. Hwang et al. (1999) collected soil boring data dated after 1990 and selected only the soil borings with depths over 15 m (50 ft.) or greater with the exception of 108 boring logs that were less than 15 m (50 ft.). Thus, of the 894 additional borings, 786 soil borings were 15 m or greater and 108 soil borings were less than 15 m.

Rix and Romero-Hudock (2006) evaluated the Ng et al. (1989) 623 interpreted soil profiles and the Hwang et al. (1990) 894 boring logs for potential use in preparing the 2005 liquefaction hazard maps. The criteria Rix and Romero-Hudock used in selecting interpreted soil profiles and boring logs are summarized below.

- i. Borings must extend to a depth of 15 m (50 ft) or greater. Thus, borings less than 15 m (50 ft.) were discarded.
- ii. The borings must include SPT-*N* values
- iii. SPT profiles located within artificial fill (af) areas were discarded.

Rix and Romero-Hudock (2006) selected a total of 623 interpreted soil profiles and boring logs that met the above criteria. Figure 5 shows the locations. However, it is not clear what specific Ng et al. (1989) interpreted soil profiles and Hwang et al. (1999) boring logs Rix and Romero-Hudock (2006) utilized in developing the 2005 liquefaction hazard maps. Therefore, for the new 2015 liquefaction hazard maps, we re-evaluated both the Ng et al. (1989) 623 interpreted soil profiles and the Hwang et al. (1990) 894 boring logs for potential use in preparing the 2015 liquefaction hazard maps and selected data using the same Rix and Romero-Hudock (2006) boring selection criteria.

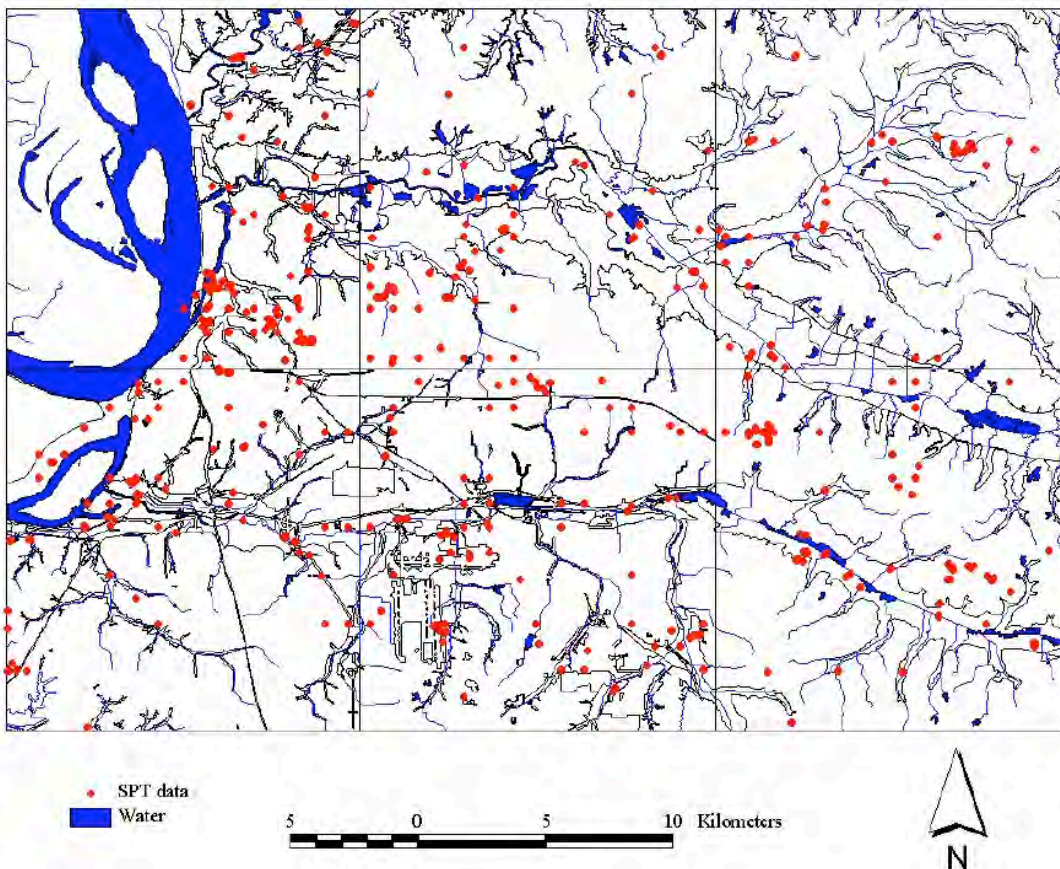


Figure 5. Location of 623 SPT profiles within six quadrangles (Rix and Romero-Hudock, 2006).

The data from the Ng et al. (1989) 623 interpreted soil profiles and the Hwang et al. (1999) 894 boring logs were included in Microsoft Excel spreadsheets. The spreadsheets contain boring locations with SPT-*N* values and USCS designations in 0.6 m (2 ft.) depth increments. Additionally, the spreadsheets also contain general soil descriptions as well as soil density, shear strength, moisture content, and groundwater information for some boring locations.

Two key changes made in the 2015 hazard maps include extended coverage area to include all of Shelby County and changes to the surficial geologic unit distribution based on an updated geologic model. The extended coverage area and the updated surficial geology are shown in Figure 6. The extended coverage area resulted in a total of 112 interpreted soil profiles from the Ng et al.(1989) database and 533 borings from the Hwang et al.(1999) that met the selection criteria.

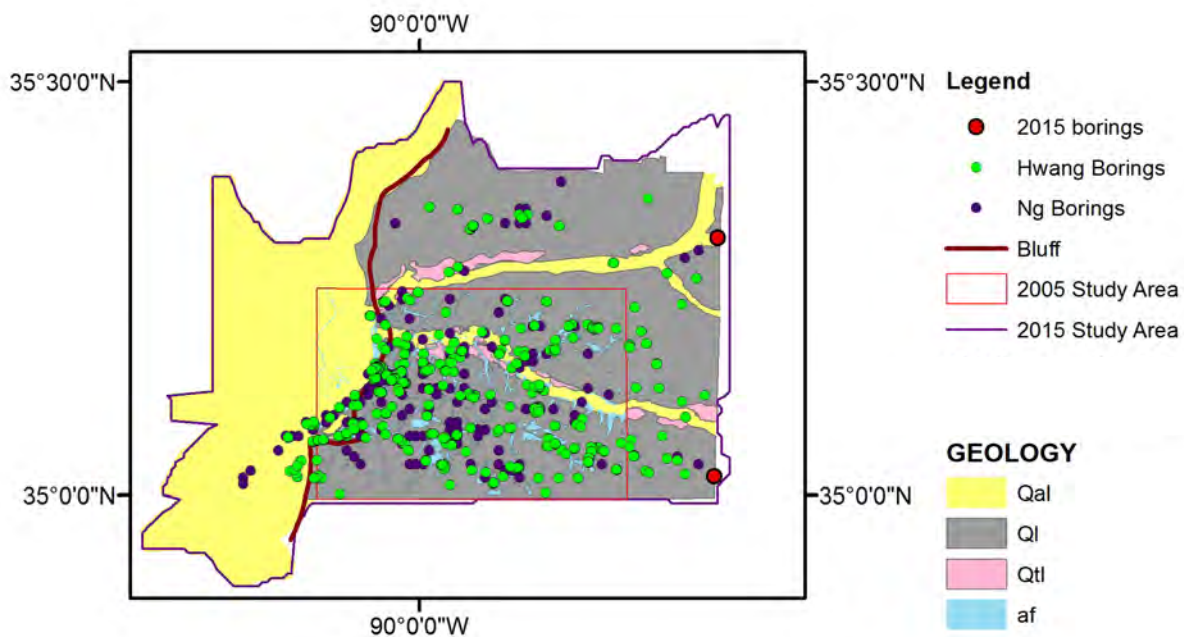


Figure 6. Location of SPT profiles for 2015 study.

One of the objectives of the present study is to add more SPT profiles. For this we have communicated with several institutions and agencies. We received total of 816 soil borings from the Memphis District of the Army Corps of Engineers, the Memphis office of Geotechnology Inc., and the Tennessee Department of Transportation (TDOT) as shown in Table 1. We utilized the same criteria adopted by Rix and Romero-Hudock (2006) to select soil borings for performing the liquefaction analysis. A total of 69 of the 816 new boring logs met all the selection criteria. The data from these 69 boring logs were included in an Excel spreadsheet in the same format as the Ng et al. (1989) and Hwang et al. (1999) Excel databases.

Table 1. Additional soil borings analyzed for present study

Agencies/Institutions	No. of soil borings received	No. of soil borings used	Reason of exclusion
Army Corp	481	0	- No complete N values to the minimum required depth of 15 m.
GEOTECH	9	0	- No complete N values to the minimum required depth of 15 m.
TDOT	326	69	- No complete N values to the minimum required depth of 15 m. - Specific boring location not available. - Located on artificial fill
Total	816	69	

Table 2 provides a summary of the SPT profiles utilized in the development of the 2015 liquefaction hazard maps. A total of 714 SPT profiles were used in this study.

Table 2. Distribution of SPT Profiles from different databases and in different surficial geologic units.

Surficial Geology	Ng et al. (1989)	Hwang et al. (1999)	Additional TDOT	Total SPT borings
Qal	16	71	5	92
Ql	92	434	64	590
Qtl	4	28		32
Total	112	533	69	714

Rix and Romero-Hudock (2006) developed liquefaction probability curves for four surface geologic units excluding artificial fill areas. Representative soil profiles were developed for each surface geologic unit, as shown in Figure 7, based on the ‘complete profiles’ available within the region of each geological unit (Rix and Romero-Hudock, 2006). From the report, it is not clear how many ‘complete profiles’ were used nor the methodology used to develop the representative soil profiles shown in Figure 7. Figure 7 shows the representative soil profiles for each of the four representative geological profiles: Qa, Qal, Ql, and Qtl. It should be noted that the new geologic model does not include Qa in the study area.

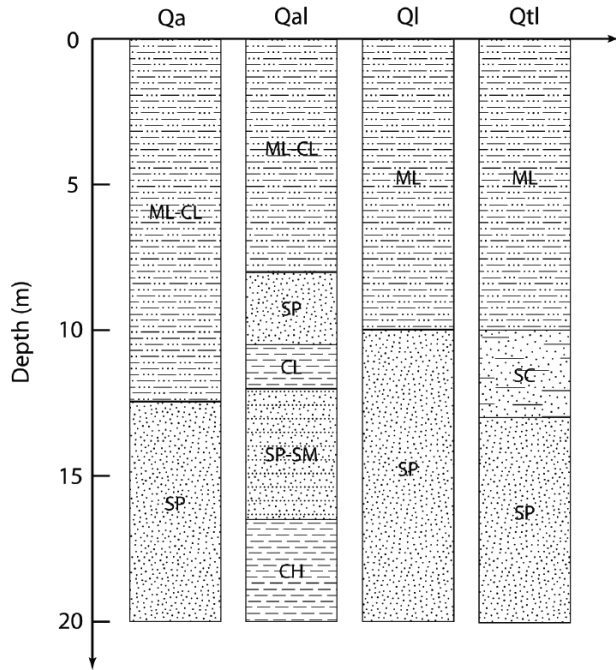


Figure 7. Representative soil profiles for each Surface Geologic unit (Rix and Romero-Hudock, 2006)

Rix and Romero-Hudock’s liquefaction analysis is based on soil profile data extending to 20 m (65 ft.). However, the Rix and Romero-Hudock criteria for selecting interpreted soil profiles and boring logs for use in the study included interpreted soil profiles and boring logs that were equal or greater than 15 m. For SPT profiles less than 20 m (65 ft.) in depth, Rix and Romero-Hudock (2006) extended the last measured standard penetration resistance value to 20 m (65 ft.) to complete the full 20 m depth soil profile. We also extended SPT profiles less than 20 m (65 ft.) in depth in a similar manner. Additionally, similar to what Rix and Romero-Hudock (2006) did, for SPT profiles with incomplete USCS designations, the USCS designation at the corresponding depth from the representative soil profile developed for each geological unit shown in Figure 7 was used.

Groundwater

Hwang et al. (1999) contained 464 soil borings that included depths at which groundwater was encountered. Based on these groundwater depths, which ranged from 2 m to 13 m, Rix and Romero-Hudock (2006) assumed a median depth to groundwater of 6 m for the entire 2005 map study area. Hwang et al. (1999) did not specify if the groundwater levels included in their database were water encountered during drilling, immediately upon completion of drilling, or a period of time after completion of drilling. Additionally, borehole cave-in depths are also not provided. As noted by Christopher and Schwartz (2006) “Unless the soils are granular with little or no fines, the water level in the boring may take days or weeks to rise to actual groundwater level. Considering the potential for cave-in and infiltration of surface water during this period and with consideration for the potential for seasonal changes in the groundwater level, a borehole is usually not the best means to get a true picture of the long-term water conditions at a site. For accurate measures of groundwater, observation wells or piezometers should be installed in the

borehole”. Therefore, we decided to utilize the results of the University of Memphis’ Groundwater Institute (GWI) 2005 groundwater study (Konduru Narsimha, 2007). GWI provided data from 254 wells and a groundwater elevation contour map (Figure 8) based on well readings recorded during the Fall 2005.

The groundwater elevation contour map and well distribution map received from GWI were in ArcGIS format. So we overlaid our interpreted soil profile and soil boring locations on the groundwater elevation contour map shown in Figure 8 and using the triangulation interpolation method, groundwater elevation was interpolated at each SPT soil profile and boring location. Since the SPT boring database did not include ground surface elevations at the SPT boring locations, ground surface elevations were estimated from Light Detection and Ranging (LiDAR) data of the Shelby County area. GWI had the LiDAR data and GWI provided us with the estimated ground surface elevations at each SPT profile location. The groundwater depth at each SPT profile location was determined by subtracting the groundwater elevation from the ground surface elevation.

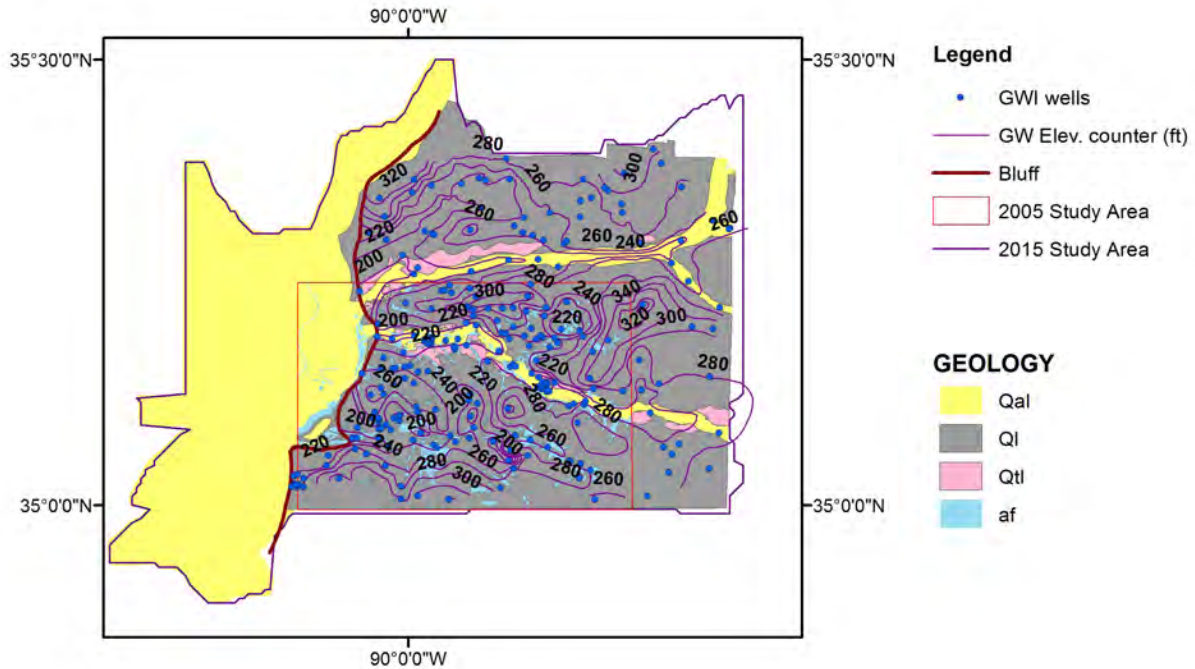


Figure 8. Well distribution and groundwater elevation map from GWI.

The 2005 GWI contour map shown in Figure 8 did not extend fully across all of Shelby County. Therefore it was not possible to interpolate groundwater elevations for those SPT profiles located near the borders of Shelby County due to incomplete contours especially along the western edge of the County where the contours were terminated at the bluff line and did not extend to the border line as shown in Figure 8. The eastern, northern, and southern edges of Shelby County consist of Q1 surface geology. The soil borings located west of the bluff line consist of Qal surface geology. The groundwater elevations of SPT profiles located outside of the 2005 GWI contour map coverage area were based on the USGS groundwater map shown in Figure 6 (Park, 1990). Since Figure 9 was not available in ArcGIS format and the number of SPT profiles

outside of the 2005 GWI contour map coverage area was less than 100, we did a visual estimation of groundwater level for the SPT profiles based on the Figure 9 groundwater contour map. The groundwater depth was calculated by subtracting the estimated groundwater elevation obtained from Figure 9 from the ground surface elevation of the SPT profile location, which as previously described, was estimated from LiDAR data of the Shelby County area.

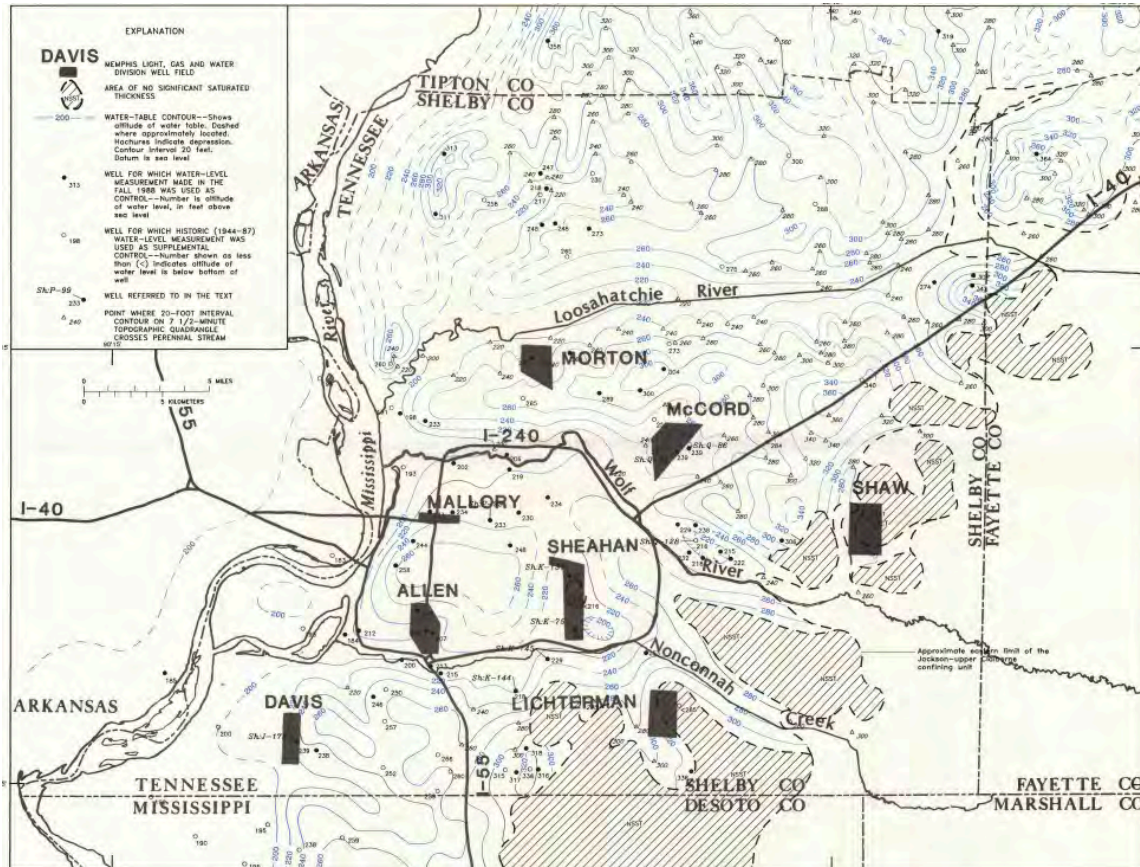


Figure 9. Altitude of the water table in the alluvium and fluvial deposits in the Memphis Area, TN, Fall 1988 (Park, 1990).

As will be discussed later in this report, use of a 6 m groundwater depth in areas with alluvium, i.e., Qal surface geology, underestimated the liquefaction hazard but overestimated the liquefaction hazard for areas with loess, i.e., Ql surface geology, where the thickness of sediments is large.

We also evaluated existing information available about fluctuations in the groundwater level in Shelby County. The USGS Water-Resource Investigations report 89-4131 (Brahana and Broshears, 1989) provides information about groundwater fluctuations in the Memphis area and some key conclusions in this report include the following:

- Seasonal variations of water level in the alluvium are typically less than 10 feet, although variations of as much as 15 feet have been reported (Plebuch, 1961; Broom and Lyford, 1981; Brahana and Mesko, 1988).
- Wells (1933), Graham (1982), and Graham and Parks (1986) reported seasonal water-

level fluctuations in the fluvial deposits in the range of 2 to 10 feet.

- Seasonal variations of nonstressed water levels are commonly less than 2 feet (Graham, 1982).
- The general conclusion in the report is that there is no significant seasonal fluctuation in water level in the Memphis area.

We also checked the seasonal variation of groundwater level by using the National Water Information System online database (NWIS, 2015). For this we selected groundwater data from three different locations for the years 2005, 2010, and 2014 and the fluctuations are presented in Table 3 and Figure 10.

Table 3. Seasonal variation in depth to groundwater level in different years (NWIS, 2015).

Locations	Year	High depth of water from ground surface (ft)	Low depth of water from ground surface (ft)	Difference between High and Low Depths (ft)	Avg. depth of water (ft) for the year	Standard Deviation of water depth for the year (ft)
Midtown (35°09'13"N 90°01'03"W")	2005	15.02 (Nov)	11.17 (May)	3.85	12.95	1.5
	2010	16.09 (Nov)	11.14 (Mar)	4.95	12.99	1.9
	2014	14.59 (Oct)	11.7 (May)	2.89	13.27	1.1
North-East (35°17'49N 89°39'44"W)	2005	22.12(Oct)	19.85 (Apr)	2.27	21.24	0.76
	2010	23.01 (Aug)	20.34 (May)	2.67	21.28	1.05
	2014	22.87 (Aug)	21.46 (Feb)	1.41	22.1	0.56
South (35°02'06"N 89°51'09"W)	2005	154.8 (Aug)	147.9 (Mar)	6.9	150.8	2.16
	2010	153.2 (Aug)	147.7 (Apr)	5.5	149.8	2.11
	2014	149 (Sep)	145.8(Mar)	3.2	147.5	1.08

From Table 3, the difference between the high and low groundwater levels is less than 10 feet, which is in general agreement with the Brahana and Broshears (1989) study. Therefore, we did not consider groundwater fluctuations in the development of the liquefaction probability curves. We only utilized the groundwater levels estimated from the 2005 Groundwater Institute contour map shown in Figure 8.

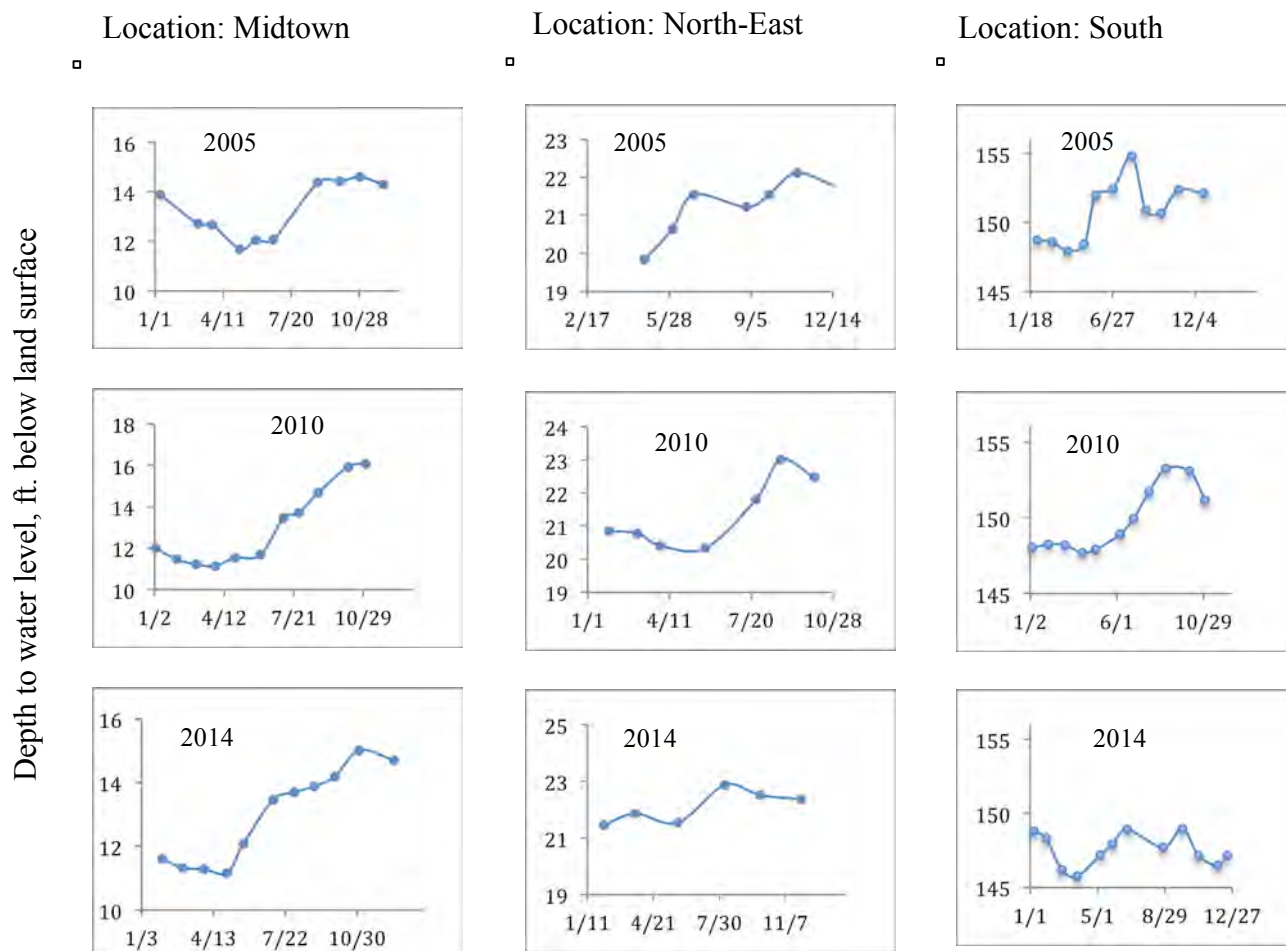


Figure 10. Seasonal variation in depth to groundwater level in different years (NWIS, 2015).

Liquefaction Probability Curves Based on SPT-N Values

Rix and Romero-Hudock (2006) developed liquefaction probability curves for each primary surficial geologic unit by (i) calculating the factor of safety (FS) against liquefaction at a given depth in the soil profile of each soil boring using the simplified procedure (Seed and Idriss, 1971); (ii) calculating liquefaction potential index (LPI) of each soil boring location using the Iwasaki et al. (1978, 1982) method; (iii) developing liquefaction probability curves (LPCs) for the probability of exceeding LPI of 5 and 15 for each primary surficial geologic unit in the Memphis area. We also utilized this three-step procedure to develop the updated LPCs. A summary of each of these three steps is subsequently provided.

Factor of safety (FS) Against Liquefaction using the Simplified Procedure

Seed and Idriss (1971) developed the simplified liquefaction evaluation procedure to compute the factor of safety (FS) against liquefaction at a given depth in a soil profile. Rix and Romero – Hudock (2006) used the simplified procedure (Seed and Idriss, 1971) to determine the factor of safety (FS) with depth within a boring or interpreted soil profile location by using the following equation:

$$FS = \frac{CRR_{7.5}}{CSR} MSF \quad (8)$$

where,

$CRR_{7.5}$ = Cyclic resistance ratio for a magnitude (M_w)=7.5 earthquake,

CSR = Cyclic stress ratio, and

MSF = Magnitude scaling factor that corrects the analysis for earthquake magnitudes other than 7.5.

CRR represents the capacity of the soil to resist liquefaction and CSR represents the earthquake induced dynamic stress exerted on the soil. In the above equation, liquefaction is expected if the factor of safety is less than 1, i.e., at depths where the earthquake induced dynamic stress exceeds the resistance of the soil against liquefaction.

Various investigators have suggested various values for MSF as shown in Table 4. The participants of the 1997 workshop on evaluation of liquefaction resistance of soils (Youd et al., 2001) recommended the ‘revised Idriss Scaling Factors’ shown in Column 3 of Table 4 as a lower bound of MSF values, which is given by

$$MSF = 10^{2.24 / M_w^{2.56}} \quad (9)$$

Rix and Romero-Hudock (2006) also used the above relation for MSF and we also utilized the ‘revised Idriss Scaling Factors’ in determining the FS against liquefaction.

Table 4. MSF defined by various investigators (Youd and Noble 1997a)

Magnitude (M)	Seed and Idriss (1982)	Idriss ^a	Ambraseys (1988)	Arango (1996)		Andrus and Stokoe (1997)	Youd and Noble (1997b)		
				Dist. based	Energy based		PL<20%	PL<32%	PL<50%
5.5	1.43	2.20	2.86	3.00	2.20	2.8	2.86	3.42	4.44
6.0	1.32	1.76	2.20	2.00	1.65	2.1	1.93	2.35	2.92
6.5	1.19	1.44	1.69	1.60	1.40	1.6	1.34	1.66	1.99
7.0	1.08	1.19	1.30	1.25	1.10	1.25	1.00	1.20	1.39
7.5	1.00	1.00	1.00	1.00	1.00	1.00	-	-	1.00
8.0	0.94	0.84	0.67	0.75	0.85	0.8?	-	-	0.73?
8.5	0.89	0.72	0.44	-	-	0.65?	-	-	0.56?

Note:?= Very uncertain values.

^a1995 Seed Memorial Lecture, University of California at Berkeley (I. M. Idriss, personal communication to T. L. Youd)

CSR represents the earthquake induced dynamic stress exerted on the soil or the seismic demand. Seed and Idriss (1971) formulated the following equation for calculation of the CSR.

$$CSR = \tau_{av} / \sigma'_{vo} = 0.65 \left(\frac{a_{max}}{g} \right) \left(\frac{\sigma_{vo}}{\sigma'_{vo}} \right) r_d \quad (10)$$

where,

a_{max} = peak ground acceleration,

g = acceleration due to gravity (9.8 m/sec²),

σ_{vo} = total vertical overburden stress,

σ'_{vo} = effective vertical overburden stress, and

r_d = stress reduction coefficient

where $r_d = 1.0 - 0.00765z$ for $z \leq 9.15$ m (z is depth) (11a)

$r_d = 1.174 - 0.0267z$ for 9.15 m $< z \leq 23$ m (11b)

These stress reduction coefficients are from Liao and Whitman (1986). Although Robertson and Wride (1998) provide r_d values for depths greater than 23 m, Youd and Idriss (2001) indicate that evaluation of liquefaction at depths greater than 23 m is beyond the depth that the simplified procedure is verified and where routine applications should be applied. The purpose of the stress reduction coefficient is to adjust the maximum shear stress that is determined at the base of a soil column that is typically assumed to be a rigid body to a soil column that is a deformable body. Thus, the stress reduction factor adjusts the maximum shear stress to represent a deformable, flexible, soil column.

Unit weight (γ) of soil layers for each boring is important to determine total vertical overburden stress (σ_{vo}) and effective vertical overburden stress (σ'_{vo}). It is not clear how Rix and Romero-Hudock (2006) determined the soil unit weights. This present study used Bowles (1977) to calculate average unit weight of each soil layer in a given soil profile based on the N values (Table 5a, 5b).

Table 5a. Empirical values for unit weight of granular soils based on the SPT-N, (Bowles, 1977).

SPT N-Value (blows/ foot)	γ (lb/ft ³)
0 - 4	70 - 100
4 - 10	90 - 115
10 - 30	110 - 130
30 - 50	110 - 140
>50	130 - 150

Table 5b. Empirical values for unit weight, of cohesive soils based on the SPT-N (Bowles, 1977).

SPT N-Value (blows/ foot)	γ sat (lb/ft ³)
0 - 4	100 - 120
4 - 8	110 - 130
8 - 32	120 - 140

CRR represents the capacity of the soil to resist liquefaction, i.e., represents the dynamic stress required to initiate liquefaction or the dynamic stress the soil can resist just before liquefying. CRR can be estimated using the results of in situ testing such as SPT, cone penetration test (CPT), shear wave velocity (V_s), and the Backer penetration test (BPT). Our present study is based on the SPT-N values for CRR calculation. Various researchers have developed SPT-based CRR relationships (Youd et.al, 2001; Cetin et al., 2004; Idriss and Boulanger, 2008; and Boulanger and Idriss, 2012). The 2005 liquefaction hazard maps are based on the Youd et.al (2001) SPT-based liquefaction triggering evaluation. We evaluated the use of the above indicated additional SPT-based liquefaction triggering relationships for obtaining LPI for

potential use in developing the liquefaction probability curves from SPT data, but stayed with the Youd et al (2001) approach for consistency with the 2005 Memphis liquefaction hazard maps.

Youd and Idriss (2001) indicate that based on a personal communication with A. F. Rauch of the University of Texas, the clean-sand $CRR_{7.5}$ versus $(N_1)_{60}$ clean sand base curve can be approximated by the following equation:

$$CRR_{7.5} = \frac{1}{34-(N_1)_{60}} + \frac{(N_1)_{60}}{135} + \frac{50}{(10(N_1)_{60}+45)^2} - \frac{1}{200} \quad (12)$$

The above equation provides the CRR for clean sand, i.e., sand with fines content less than 5%. Thus, in the above equation $(N_1)_{60}$ is the corrected SPT-N value for a clean sand. For sands with fines content greater or equal to 5%, Idriss and Seed proposed the following equations for correcting $(N_1)_{60}$ to an equivalent clean sand value of $(N_1)_{60cs}$ (Youd and Idriss 2001):

$$(N_1)_{60cs} = \alpha + \beta (N_1)_{60} \quad (13)$$

where,

$$\begin{aligned} \alpha &= 0 && \text{for } FC \leq 5 \% \\ \alpha &= \exp \left[1.76 - \left(\frac{190}{FC^2} \right) \right] && \text{for } 5\% < FC < 35 \% \\ \alpha &= 1.2 && \text{for } FC \geq 35\% \\ \beta &= 1.0 && \text{for } FC \leq 5 \% \\ \beta &= \left[0.99 + \left(\frac{FC^{1.5}}{1000} \right) \right] && \text{for } 5\% < FC < 35 \% \\ \beta &= 1.2 && \text{for } FC \geq 35\% \end{aligned}$$

where FC is fine contents. Note that for $FC \leq 5$, $(N_1)_{60cs} = (N_1)_{60}$

Rix (2001) used the following SPT relationship for M_w 7.5:

$$CRR_{7.5} = \frac{1}{34-(N_1)_{60cs}} + \frac{(N_1)_{60cs}}{135} + \frac{50}{(10(N_1)_{60cs}+45)^2} - \frac{1}{200} \quad (14)$$

where $(N_1)_{60cs}$ is the equivalent clean sand standard penetration resistance. The equivalent clean sand standard penetration resistance is obtained by correcting the measured standard penetration resistance (N_m) for effective overburden stress, hammer energy ratio, borehole diameter, rod length, samplers with or without liners, and fines content. However, due to limited information available from the SPT data included in the boring logs, Rix (2001) only included corrections for effective overburden stress. So, $(N_1)_{60}$ is obtained from the measured standard penetration resistance (N_m) using,

$$(N_1)_{60} = N_m C_N \quad (15)$$

where C_N is the correction for effective overburden stress obtained from

$$C_N = (P_a / \sigma'_{vo})^{0.5} \quad (\text{Liao and Whitman, 1986}) \quad (16)$$

where P_a = atmospheric pressure in same units as σ'_{vo} or P_a is 100 kPa if σ'_{vo} is in kPa.

C_N should not exceed 1.7 (Youd et al., 2001).

Based on the Rix and Romero-Hudock (2006) study, the present study also approximated the fines content from the Unified Soil Classification System (USCS) using Table 6.

Table 6. Assumed fines content based on USCS soil type

USCS Soil Type	Assumed Fines Content (%)
GW, GP, SW, SP	0
GW-GM, GW-GC, GP-GM, GP-GC, SW-SM, SW-SC, SP-SM, SP-SC	5
GC, GM, GC-GM, SC, SM, SC-SM	12
CH, CL, MH, ML, OL, OH, CL-ML	50

The factor of safety was determined against liquefaction at 0.6 m (2 ft.) increment depths at each interpreted soil profile or individual boring location. After the factor of safety values with depths were determined, the next phase of the analysis consisted of determining the liquefaction potential index (LPI) at each interpreted soil profile or individual boring location.

Liquefaction Potential Index (LPI)

Seed and Idriss (1971) developed the simplified liquefaction evaluation procedure to compute the factor of safety (FS) against liquefaction at a given depth in a soil profile. Thus, the simplified procedure predicts triggering of liquefaction at a specific depth but it does not predict the severity of liquefaction manifestation at the ground surface. Since liquefaction manifestation at the ground surface better correlates to liquefaction damage, Iwasaki et al. (1978) proposed the LPI procedure to better characterize the damage potential of liquefaction.

The liquefaction potential index (LPI) was originally proposed by Iwasaki et al. (1978, 1982) based on historic liquefaction at 63 liquefied sites and 22 non-liquefied sites impacted by six earthquakes that struck Japan between 1891 and 1978. This method has since been adopted to evaluate liquefaction potential in North America (Luna and Frost 1998; Toprak and Holzer 2003; Holzer et al. 2006; Baise et al., 2006). The LPI defined by Iwasaki et al. (1978, 1982) can be expressed as follows:

$$LPI = \int_{0 \rightarrow 20} F(z) w(z) dz \quad (17)$$

where

z = depth (0~20 m),

dz = the differential increment of depth,

$F(z)$ = severity, which is a function of the Factor of Safety (FS) and is determined by

$$F(z) = 1 - FS \quad \text{for } 0 \leq FS \leq 1$$

$$F(z) = 0 \quad \text{for } FS > 1$$

and $w(z)$ = weighting function = $10 - 0.5z$.

Note that the LPI is determined to a maximum depth of 20 m. Also note that the weighting function incorporates the greatest effect of liquefaction to be at the ground surface, i.e., $w(0)=10$, and the least effect at a depth of 20 m, i.e., $w(20)=0$.

The LPI was determined at each soil boring location for a_{max} values 0.1 g, 0.2 g, 0.3 g, 0.4 g, and 0.5 g and M_w values of 6.0, 6.5, 7.0, 7.5, and 8.0. Thus, a total of 25 combinations of a_{max} and M_w were used to evaluate the distribution of LPI at each soil boring or interpreted soil profile location.

Liquefaction Probability Curves

After the determination of LPI at each boring location, the distribution of LPI was determined within each of the following three surficial geologic units in Memphis: Holocene alluvial flood plain deposits (Qal), late Pleistocene loess deposits (Ql), and Pleistocene loess-covered terrace deposits (Qtl). The geologic unit of each individual soil boring location was determined by overlaying the location of each individual soil boring location over the geologic unit map. The estimated LPI values for each geologic unit were evaluated for each combination of a_{max} and M_w as shown in Figure 11 to obtain the distribution of LPIs for a given geologic unit. For example, Figure 11 shows the histogram of the LPI for unit Qal and for $a_{max} = 0.3$ g and $M_w = 8.0$ for all 92 individual boring logs that were located within the Qal geologic unit. The distribution of LPI was determined for each of the 25 combinations of a_{max} and M_w for each surficial geologic unit.

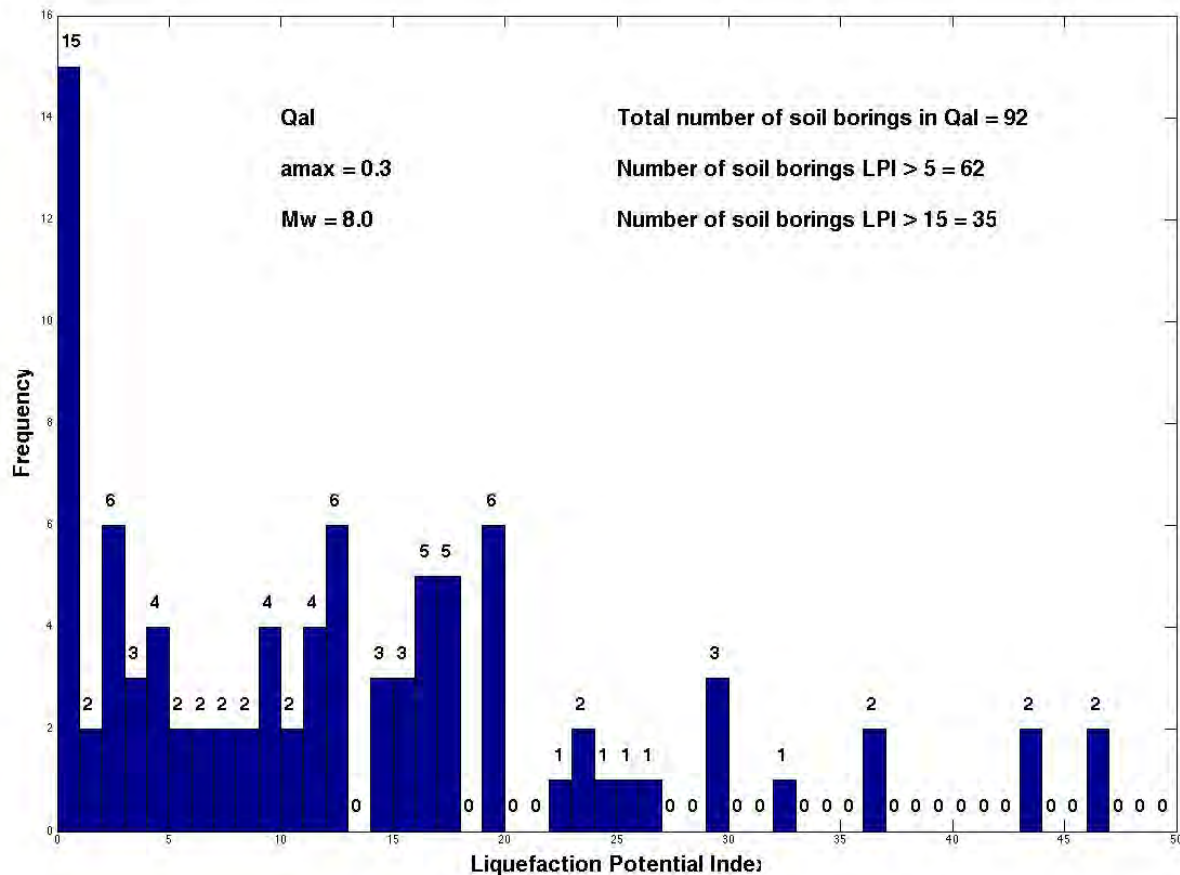


Figure 11. Histogram of LPI for SPT data for Unit Qal, $a_{max} = 0.3$ g and $M_w = 8.0$.

Similar to the Rix and Romero-Hudock (2006) study, this study is based on the threshold values proposed by Iwasaki et al. (1978, 1982). Iwasaki et al. (1978, 1982) proposed, on the basis of SPT data, that at $LPI < 5$, severe liquefaction is unlikely, and that at $LPI > 15$, severe liquefaction is likely. Based on CPT soundings, Toprak and Holzer (2003) and Holzer (2010, personal communication) recommended $LPI > 12$ and $LPI > 5$ for predicting lateral spreading and ground cracking (severe hazard) and surface manifestations such as sand boils (moderate hazard),

respectively. Therefore, the primary difference between SPT-based findings and the CPT-based findings is that the threshold for severe liquefaction hazard is 15 based on SPT data and 12 based on CPT. We evaluated these two severe hazard threshold values by comparing liquefaction probability curves between the SPT and CPT data for $LPI > 12$ as well as $LPI > 15$ to determine which threshold value to adopt for the updated hazard maps, but stayed with the Iwasaki et al. (1978, 1982) approach for consistency with the 2005 Memphis liquefaction hazard maps (Rix and Romero-Hudock, 2006).

Using the LPI distributions shown in Figure 11, it is possible to calculate the probability of exceeding LPI values of 5 and 15, which are the lower bounds of “moderate” and “major” liquefaction, respectively, based on the results of Iwasaki et al. (1978,1982) and Toprak and Holzer (2003). For example, using the histogram in Figure 11, the probability of exceeding LPI values of 5 can be determined as

$$P[LPI > 5] = \frac{62 \text{ borings exceeding LPI of } 5}{92 \text{ total soil borings}} * 100 = 67 \%$$

and $\frac{a_{max}}{MSF} = \frac{0.3}{10^{2.24}/8^{2.56}} = 0.354$

This combination of $P[LPI > 5]$ of 0.67 and a_{max}/MSF of 0.354 is shown as a single point in Figure 12a for geologic unit Qal. Figure 12a shows data points for all 25 combinations of a_{max} and M_w that were used to evaluate the distribution of LPI at each soil boring or interpreted soil profile location.

Similarly, the probability of exceeding LPI values of 15 can be determined as

$$P[LPI > 15] = \frac{35}{92} * 100 = 38 \%$$

and $\frac{a_{max}}{MSF} = \frac{0.3}{10^{2.24}/8^{2.56}} = 0.354$.

This combination of $P[LPI > 15]$ of 0.38 and a_{max}/MSF of 0.354 is shown as a single point in Figure 12b for geologic unit Qal. Figure 12b shows data points for all 25 combinations of a_{max} and M_w that were used to evaluate the distribution of LPI at each soil boring or interpreted soil profile location.

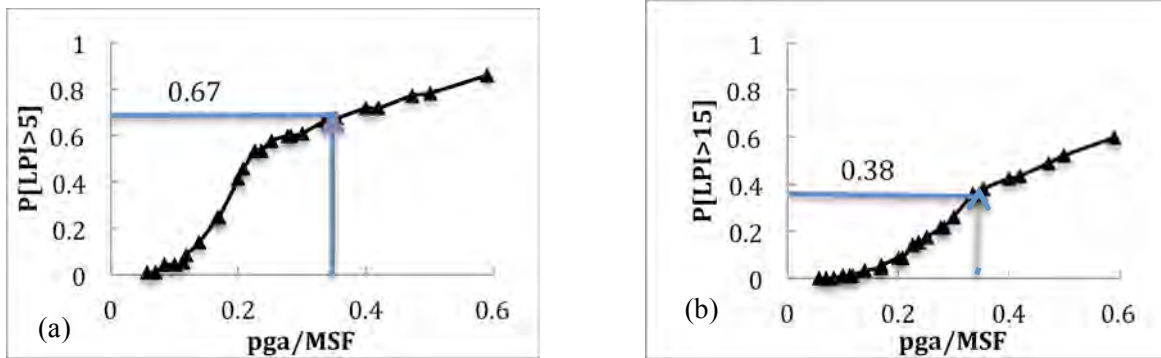


Figure 12 (a) Probability of $LPI > 5$; (b) Probability of $LPI > 15$ for Qal, $a_{max} = 3g$, and $M_w = 8$

Figures 13a and 13b show the probability curves of exceeding LPI values of 5 and 15, respectively, as a function of the adjusted peak ground acceleration (a_{max}/MSF) for each geologic unit based on the SPT data. Thus, the primary outcomes of the present study are the three liquefaction probability curves shown in Figure 13a representing $P[LPI>5]$ (moderate liquefaction potential) for each of the three surficial geologic units in Memphis and the three liquefaction probability curves shown in Figure 13b representing $P[LPI>15]$ (severe liquefaction potential) for each of the three surficial geologic units in Memphis.

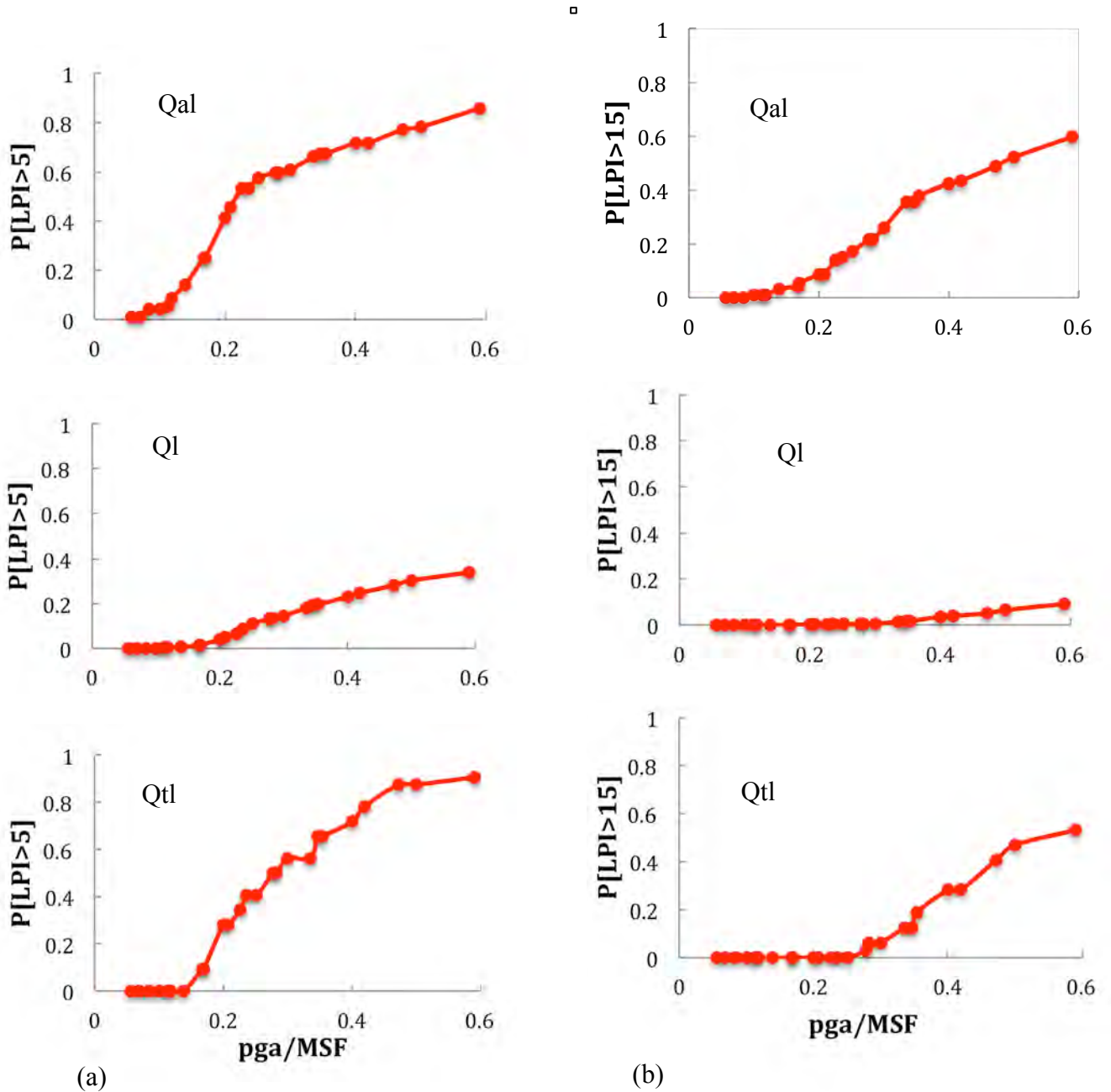


Figure 13 (a) Probability of $LPI > 5$; (b) Probability of $LPI > 15$ for each geologic unit

Comparison of the Current LPCs and the 2005 LPCs

The key changes included in the 2015 LPCs compared to the 2005 LPCs are the addition of new SPT profiles, use of the 2012-2013 Memphis geologic model, and use of the GWI 2005 groundwater depth model. 2005 liquefaction maps were based on uniform water depth of 6 m for all the study area. Use of a 6 m groundwater depth in soil borings for alluvium underestimated liquefaction hazard and overestimated hazard for loess. Since groundwater depth is very important factor for liquefaction analysis, we have adopted a newer groundwater model based on the Groundwater Institute 2005 study. Based on the newer model, we have assigned groundwater depth to each soil boring for liquefaction analysis. Comparisons of LPCs for $P[LPI > 5]$ (Figure 14a) and $P[LPI > 15]$ (Figure 14b) show that for Q_{al} the updated curves are higher than 2005 Q_{al} curves where as for Q_l the curves are lower which is logical due to the groundwater depth associated with thickness of sediments. For Q_{tl} the curves are not much changed.

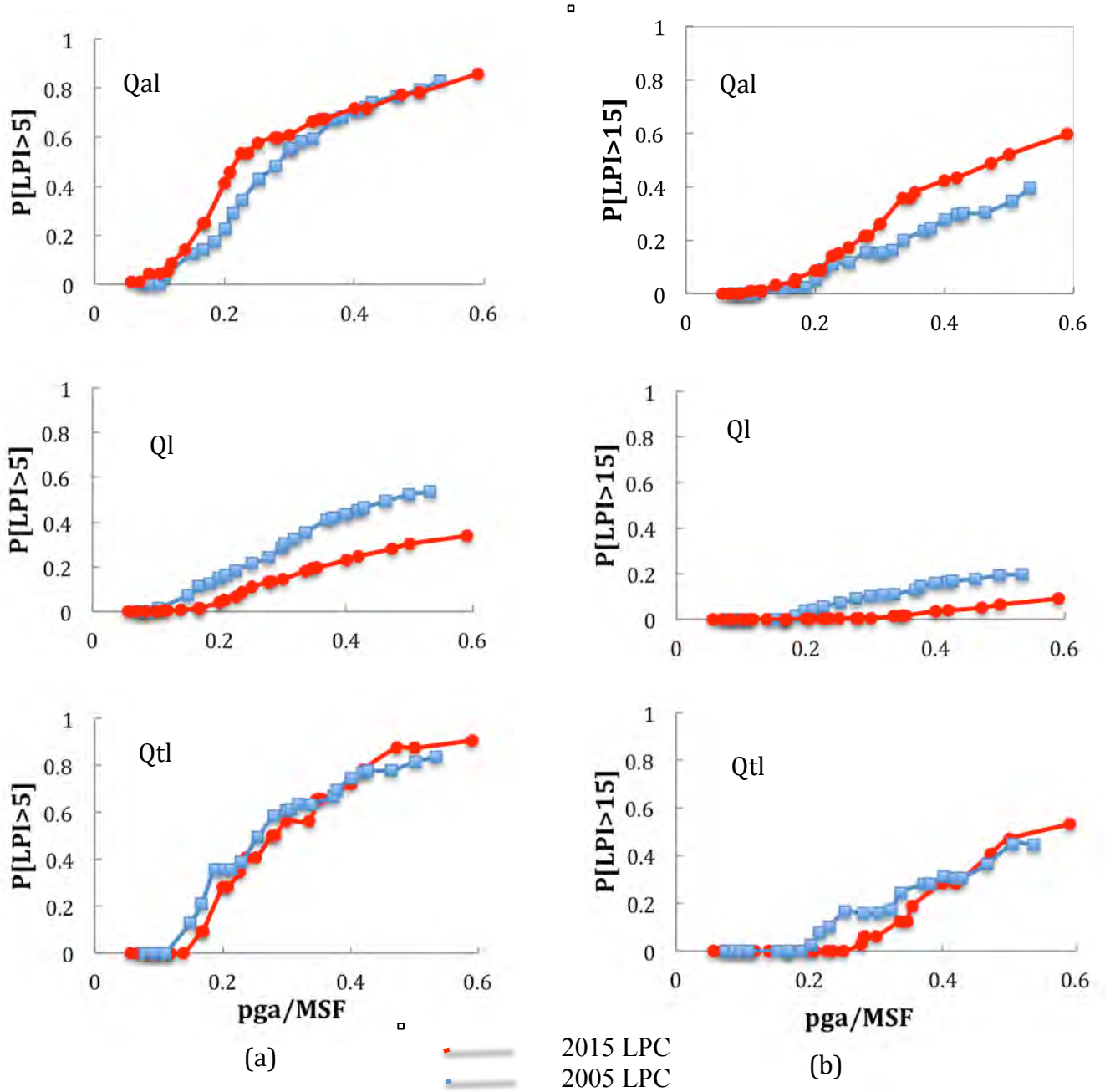


Figure 14. Comparison of 2005 and 2015 liquefaction probability curves for *Qal*, *Ql*, and *Qtl* for (a) $P[LPI>5]$ and (b) $P[LPI>15]$.

Liquefaction Probability Curves based on Cone Penetration Test (CPT)

Rix and Romero-Hudock (2006) used a very limited (only 18) number of CPT profiles (Table 7) to carry out liquefaction analysis in the area. The limited number of CPT profiles may not show the heterogeneity of the area. Rix and Romero-Hudock used a numerical method to generate CPT profiles to capture the heterogeneity of the various geologic units. A stochastic approach

was used to simulate CPT profiles that incorporate the statistics of the measure profiles. The mean, standard deviation, and autocorrelation function were used to produce simulated profiles. A total of 1200 simulated profiles of cone tip resistances (q_t) and sleeve resistance (f_s) were generated for each geologic unit. The LPI for each stochastically simulated profile was calculated and liquefaction probability curves were developed based on such LPIs.

Table 7. Number of CPT profiles used in 2005 study

Geologic Unit	Number of CPT Profiles
Qal	0
Qa	12
Ql	4
Qtl	2
Total	18

Rix and Romero-Hudock (2006) generated liquefaction probability curves based on SPT data as well as CPT data. They performed the liquefaction hazard integral calculations using Equation 7 for each soil type liquefaction probability curve as well as for each data type, i.e., SPT and CPT. Rix and Romero-Hudock (2006) combined the SPT and CPT based liquefaction hazard integral calculation results for each surface geology type by using the weighted averaging of Rix and Romero-Hudock (2006) of 2/3 and 1/3 for the SPT-based and CPT-based liquefaction hazard integral calculation results, respectively. Rix and Romero-Hudock (2006) indicate that the assignment weight of 2/3 to the SPT data and 1/3 to the CPT data was an attempt to properly balance the results based on a large number of SPT profiles of uncertain quality and small number of CPT profiles of high quality. A higher weight was assigned to the SPT data because “the more plentiful SPT data better captures the heterogeneity within each geologic unit (Rix and Romero-Hudock, 2006) and was an attempt to model (epistemic) uncertainty” (Cramer et al., 2008). However, Rix and Romero-Hudock (2006) admit that the weight assignment was “somewhat arbitrary and other combinations can be justified.”

To update the LPCs based on CPT profiles, we evaluated nine additional CPT profiles available from USGS (Table 8). Instead of using simulated profiles based on limited measured profiles we decided to determine the feasibility of using the actual CPT profiles. However, even with the addition of nine CPT new profiles, as shown in Table 8, the currently available 27 CPT profiles do not fully cover the study area. Therefore, the updated CPT data set was still insufficient and the updated SPT liquefaction hazard curves were much improved, so full weight was given to the 2015 SPT curves and no weight to the 2015 CPT curves. In summary, in the present study, we did not incorporate LPCs based on CPT profiles to prepare the liquefaction hazard maps.

Table 8. Number of CPT profiles available for present study

Geologic Unit	Number of CPT Profiles
Qal	18
Ql	6
Qtl	3
Total	27

Summary on Geotechnical Analyses

The main objective of geotechnical analyses portion of the research is to update the liquefaction probability curves to prepare the new liquefaction hazard maps. The key changes included in the updated in the updated liquefaction probability curves includes the addition of new SPT boring data, use of the 2012-2013 Memphis geologic model, and use of the GWI 2005 groundwater level model. Additionally, the updated liquefaction hazard maps are generated with liquefaction probability curves based on SPT data only and do not include the very limited CPT profiles currently available within the study area.

Hazard Model Update

As part of this study we updated the seismic hazard model to the 2014 USGS NSHMP model of Petersen et al., 2014. The 2014 NSHMP model has additional sources in the central US that tend to raise seismic hazard. The 2014 model also has updated attenuation models and weights that tend to lower predicted ground motions and hence seismic hazard. The overall result of these changes from the 2008 NSHMP model is that our 2015 probabilistic urban seismic hazard maps show similar hazard (within 5-10%) to the 2013 probabilistic seismic hazard maps of Cramer et al. (2014) but lower 2015 scenario seismic hazard maps by 0.05 – 0.1 g compared to the 2013 scenario seismic hazard maps of Cramer et al. (2014).

2015 Memphis Urban Hazard Maps

Revised Memphis urban seismic and liquefaction hazard maps have been produced for both probabilistic and scenario cases. Probabilistic maps are for 2%, 5%, and 10% exceedance in 50 years. Scenario maps have been generated for a M7.5 on the southwest arm of the New Madrid seismic zone (consistent with the results of Cramer and Boyd, 2014), a M6.2 at Marked Tree, AR (consistent with the 1843 earthquake at that location), a M7.0 at Marianna, AR (consistent with the paleoseismic work of Tuttle et al., 2006), and a M6.0 and M6.5 on the Meeman-Shelby Fault near downtown Memphis (consistent with Hao et al., 2013). Seismic hazard maps are for peak ground acceleration (PGA), 0.2 s spectral acceleration (Sa), 0.3 s Sa, and 1.0 s Sa. Liquefaction hazard maps are for Liquefaction Potential Index (LPI) > 5 (moderate or greater hazard) and LPI > 15 (severe hazard). Simplified seismic and liquefaction hazard maps have also been derived for use by a non-technical user community.

The Cramer et al. (2014) geology model with Vs observation constraints has been used in developing the 2015 Memphis urban hazard maps. That geology model used more detailed shallow layers with offsets (faults or erosional features) and is expanded to cover all of Shelby County. Shallow layer Vs interpretation has been constrained by Vs observations that show the slowest Vs layer (<200 m/s) is limited to about 10 m or less (Romero and Rix, 2001), which provides a more uniform hazard between the loess covered upland and the thick alluvial Mississippi River lowlands (Cramer et al., 2014). The liquefaction hazard maps use the surface geology map for the study area in a GIS to “cookie cutter” liquefaction hazard from calculations

for each surface geology type (differing liquefaction potentials). Figure 15 shows the surface geology map used in the generation of the 2015 liquefaction hazard maps.

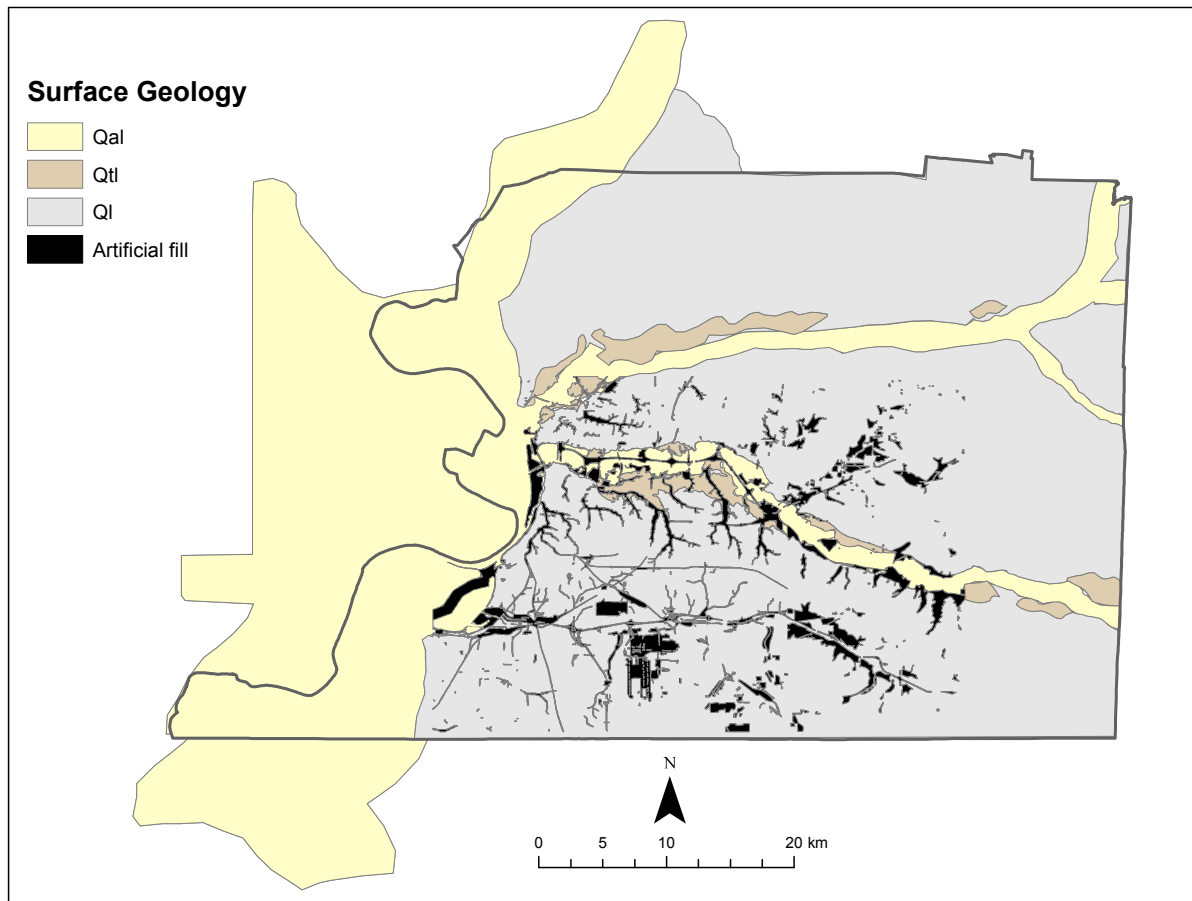


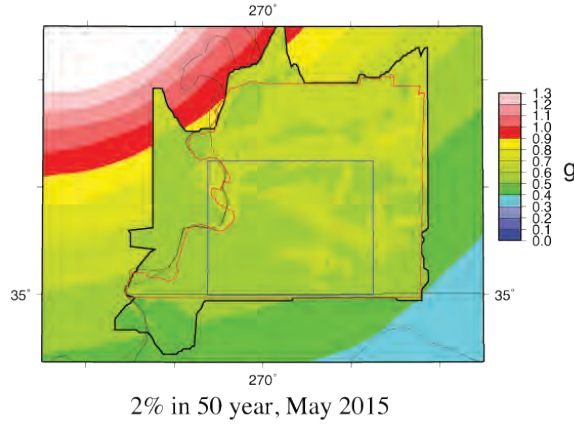
Figure 15. Surface geology map used to generate liquefaction hazard maps in a GIS. Artificial fill areas are areas requiring special study to determine the engineering character of the fills.

Figure 16 presents probabilistic hazard maps for 2% in exceedance in 50 years. Shown in Figure 16 are seismic hazard maps for PGA, 0.2 s Sa, and 1.0 s Sa plus liquefaction hazard maps for LPI > 5 (moderate or greater hazard) and LPI > 15 (severe hazard). The seismic hazard ranges from 0.4 to 0.7 g for PGA, 0.5 to 1.0 g for 0.2 s, and 0.4 to 0.8 g for 1.0 s. Compared to the equivalent 2014 NSHMP maps shown in the background in Figure 16, these 2015 Memphis urban seismic hazard maps are up to 40% and 60 % lower for PGA and 0.2 s Sa, respectively, due to nonlinear soil response, and 60% to 100% higher for 1.0 s Sa due to soil resonance (nonlinear soil response is reduced at long period). 2015 Memphis urban liquefaction hazard at 2% in 50 years ranges from 40% to over 90% for moderate or greater liquefaction hazard (LPI > 5) and from less than 10% to 70% for severe liquefaction hazard (LPI > 15). The upland areas have lower liquefaction hazard than the lowland areas.

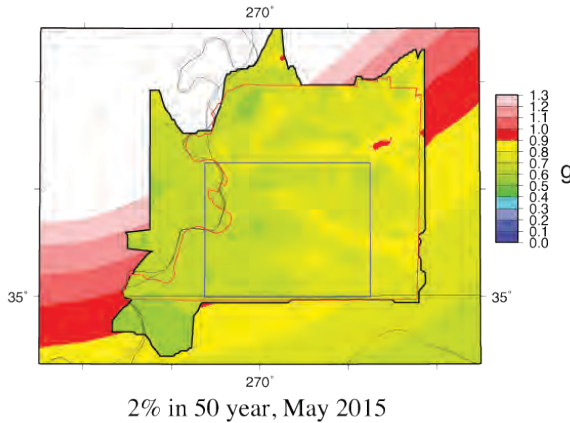
Figure 17 presents scenario hazard maps for a M7.5 earthquake on the southwest arm of the New Madrid seismic zone. This M7.5 scenario is the most likely damaging earthquake for the Memphis area. The scenario seismic hazard ranges from 0.2 to 0.4 g for PGA and 0.2 s Sa, and

0.1 to 0.6 for 1.0 s Sa. These 2015 ground motion maps are 0.05 to 0.1 g lower than the 2013 equivalent maps due to the reduction in predicted ground motions from the 2014 NSHMP suite of attenuation relations and weights with respect to the 2008 NSHMP suite of attenuation relations and weights. The scenario liquefaction hazard ranges from less than 10% to 70 % for moderate or greater liquefaction (LPI < 5) and from less than 10% to 50% for severe liquefaction (LPI < 15).

Memphis Urban PGA Hazard



Memphis Urban 0.2s Sa Hazard



Memphis Urban 1.0s Sa Hazard

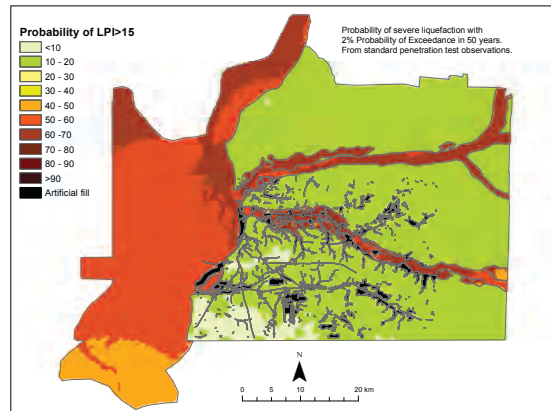
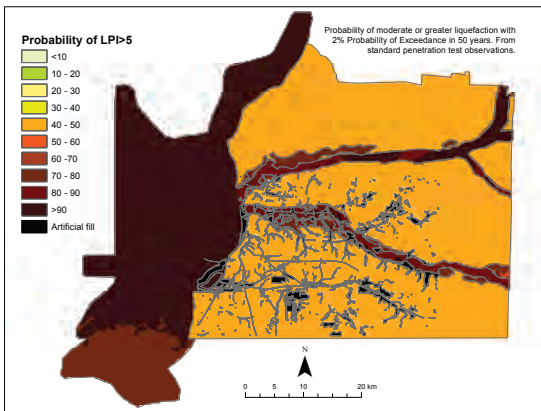
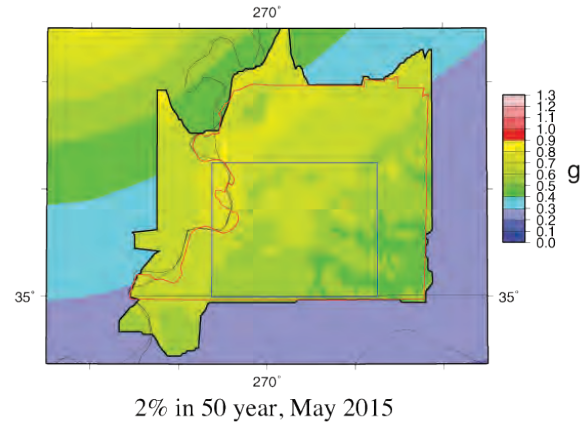
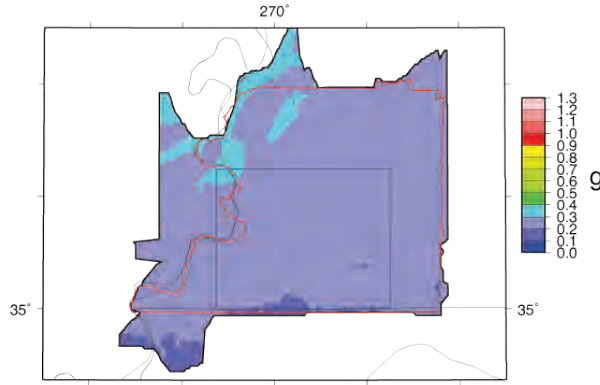


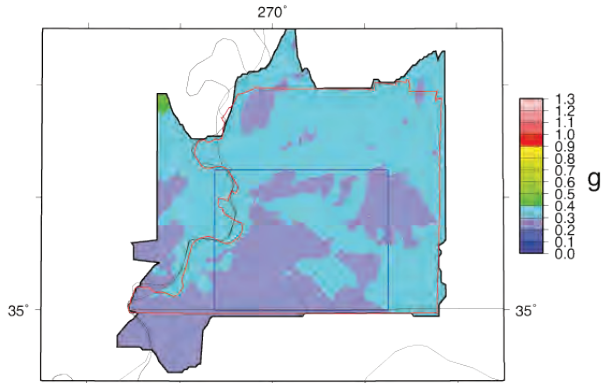
Figure 16. Seismic and liquefaction hazard maps for 2% in 50-year hazard. The blue rectangle is the 2004 six-quadrangle study area and the red polygon is Shelby County.

Memphis Urban PGA Hazard



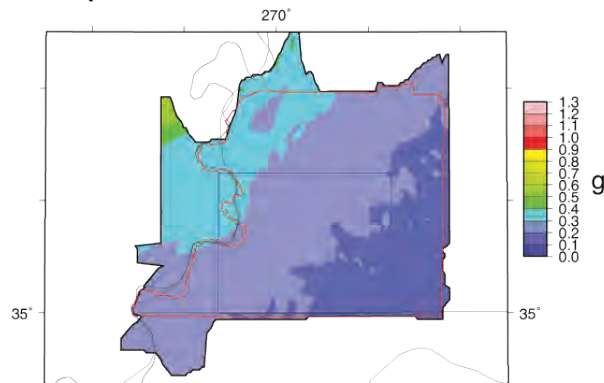
NMSW 7.5, Sept 2015

Memphis Urban 0.2s Sa Hazard



NMSW 7.5, Sept 2015

Memphis Urban 1.0s Sa Hazard



NMSW 7.5, Sept 2015

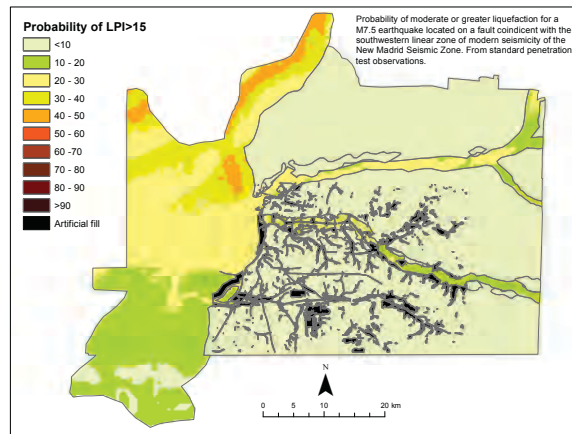
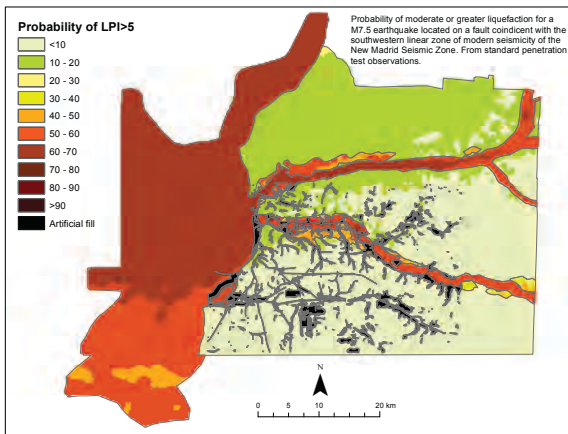


Figure 17. Seismic and liquefaction hazard maps for a M7.5 on the southwest arm of the New Madrid seismic zone. The blue rectangle is the 2004 six-quadrangle study area and the red polygon is Shelby County.

The pattern of observed liquefaction features trailing off upstream in the Wolf River (Broughton et al., 2001) is similar to the scenario LPI > 5 liquefaction hazard reduction going upstream in Figure 17, suggesting that the scenario liquefaction maps might be consistent with the observations. However, in the Loosahatchie River where liquefaction features are only observed near the mouth of the river and not upstream (Broughton et al., 2001), the scenario liquefaction hazard maps may overstate the hazard due to insufficient geotechnical sampling of the Loosahatchie River sediments.

Figure 18 presents scenario PGA hazard maps for the other scenario earthquakes of this study. The M6.2 Marked Tree scenario PGAs range from less than 0.1 to 0.2 g and the M 7.0 Marianna scenario ranges from 0.1 to 0.2 g, both of which are less than the M7.5 New Madrid scenario (0.2 to 0.4 g). However, local smaller magnitude earthquakes can have significantly higher PGAs over a limited area as demonstrated by the Meeman-Shelby Fault scenarios. The Meeman-Shelby Fault M6.0 scenario PGAs range from 0.1 to 0.5 g and the M6.5 scenario PGAs

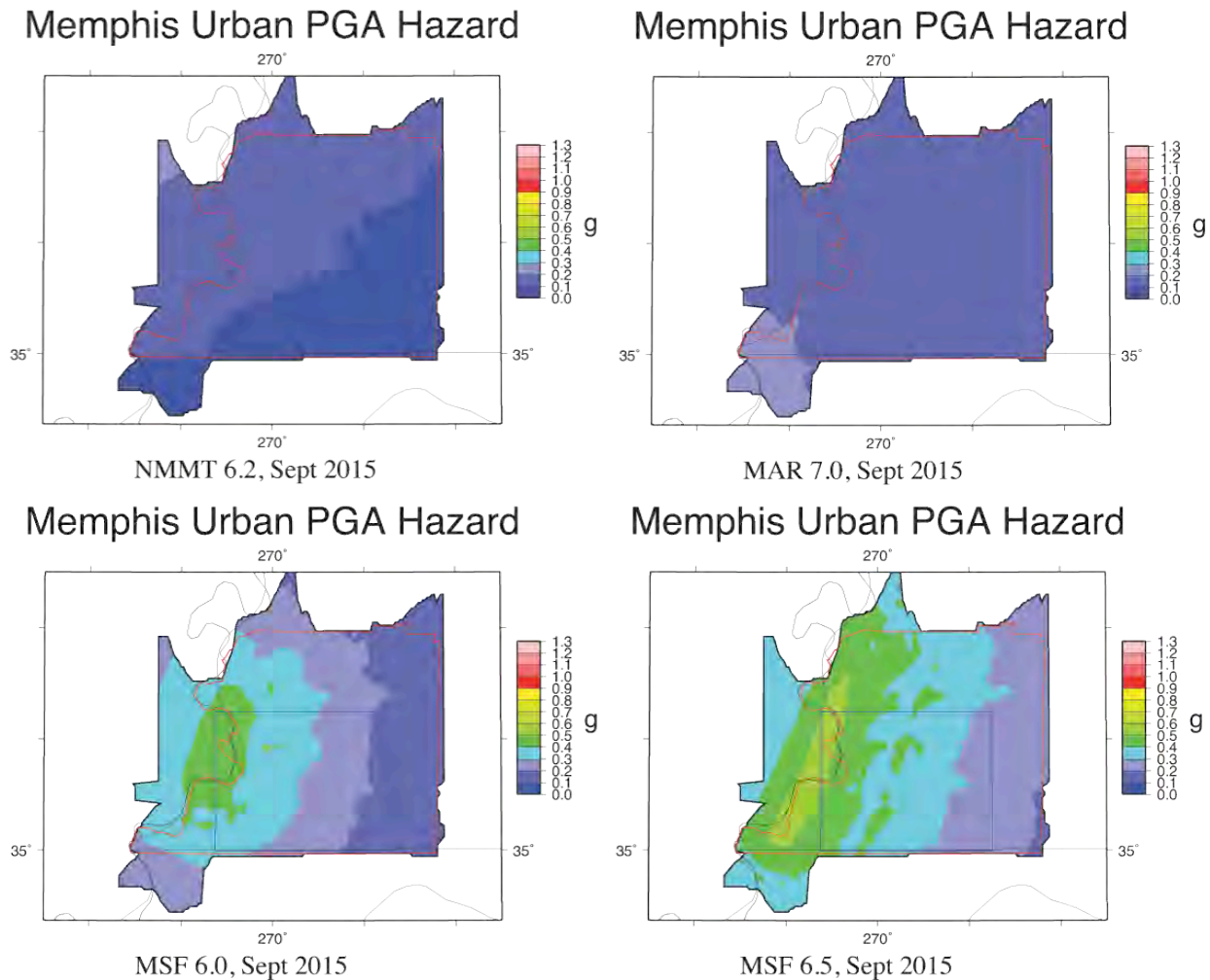


Figure 18. Scenario PGA hazard maps for a M6.2 near Marked Tree, AR (upper left), a M7.0 near Marianna, AR (upper right), a M6.0 on the central segment of the Meeman-Shelby Fault (lower left), and a M6.5 on the Meeman-Shelby Fault (lower right). The blue rectangle is the 2004 six-quadrangle study area and the red polygon is Shelby County.

range from 0.2 to 0.6 g, 0.1 g higher. Because the Meeman-Shelby Fault passes within 10 km of downtown Memphis, the high PGAs affect the heart of Memphis. Fortunately, an occurrence of a Meeman-Shelby scenario is very rare with a recurrence rate for M6 earthquakes on the order of 5,000 to 10,000 years.

Figure 19 presents simplified urban hazard maps based on the 5% in 50 year PGA and LPI > 5 (probability of surface manifestation of liquefaction) technical hazard maps. In these maps severe shaking hazard represents PGA exceeding 0.25 g, and liquefaction hazard is represented as low for less than 30% probability of surface manifestations, as severe for greater than 60 % probability of surface manifestations, and moderate between these two levels. 5% in 50 year PGA hazard was chosen because it represents up to the 60 percentile ground motions for New Madrid M7 earthquakes, which occur on average about every 500 years. 10% in 50 year hazard only represent up to the 35 percentile ground motions from the New Madrid M7s and does not cover median expected ground motions from these earthquakes. Also probabilistic ground motion hazard represents the hazard from all modeled earthquake sources in the region instead of just one earthquake, albeit the most probable one.

Memphis Urban Shaking Hazard Memphis Urban Liquefaction Hazard

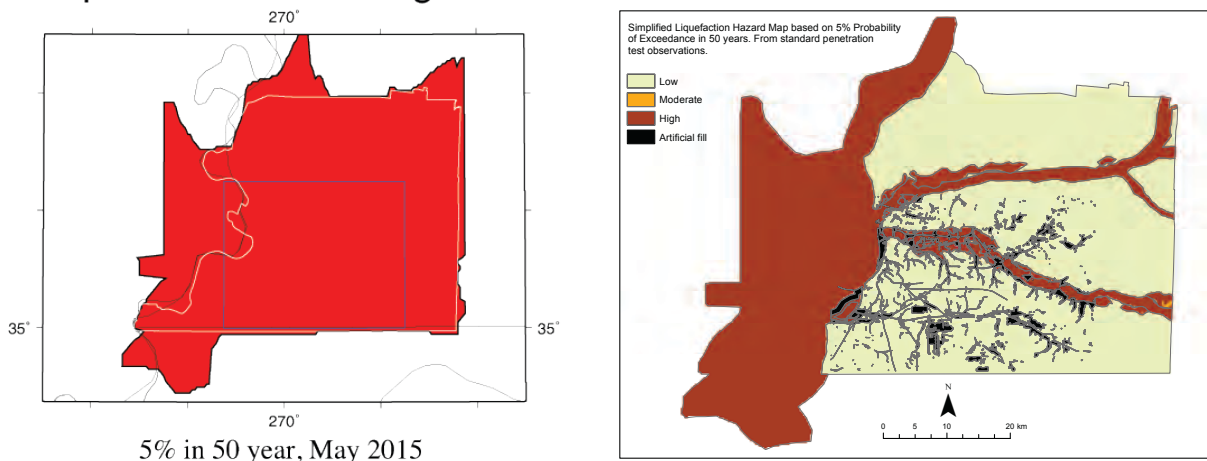


Figure 19. Simplified shaking and liquefaction hazard maps based on 5% in 50-year hazard. The blue rectangle is the 2004 six-quadrangle study area and the white polygon is Shelby County.

Workshop

On July 28, 2015 a Memphis Area Earthquake Hazards Mapping Project (MAEHMP) workshop was held to present the 2015 urban hazard maps to the user community and to gain their feedback on usable products and future directions (see Appendix A for workshop agenda). The workshop was held at the Big Cypress Lodge facilities in the Bass Pro Pyramid. The 137 workshop participants represented a diverse group of stakeholders, including academic and government scientists, local utility managers and engineers, local and state emergency management officials, and engineering and geotechnical firms, etc. (see Appendix B for list of attendees). Topics covered during the workshop included the earthquake hazard setting in the Memphis area, understanding urban earthquake hazard maps, why liquefaction hazard maps are important, using the maps and mitigation efforts, who needs to know about and use hazard maps,

and user community feedback as to hazard mapping needs. The lunch speaker was Dr. David Johnston from GNS Science New Zealand, and the liquefaction guest presenters were Dr. Russell Green from Virginia Tech and Ashraf Elsayed from the local company Geotechnology, Inc. Sponsors of the workshop were the West Tennessee Seismic Safety Commission, the U. S. Geological Survey, the Mid-South Association of Contingency Planners, state Farm Insurance, and the Center for Earthquake Research and Information.

The MAEHMP Technical Working Group had an initial in-person meeting September 9, 2014, and a semi-annual in-person meetings April 10, 2015 plus planning and progress conference calls October 16, 2014, November 20, 2014, January 20, 2015, February 20, 2015, April 10, 2015, May 14, 2015, May 29, 2015, June 26, 2015, and July 16, 2015. The one-day in-person meetings were held at the CERI at the University of Memphis. These conference calls and meetings allowed the PIs to brief TWG participants on the progress of the study and for the TWG to offer critiques and guidance to the PIs.

Most presentations from the workshop are available at <https://umdrive.memphis.edu/ccramer/public/MemhisHazMaps/2015WorkshopPresentations>

References

- Ambraseys, N. N., 1988, Engineering seismology, *Earthquake Engrg. and Struct. Dynamics*, 17, 1–105.
- Andrus, R. D., and Stokoe, K. H., II., 1997, Liquefaction resistance based on shear wave velocity, *Proc., NCEER Workshop on Evaluation of Liquefaction Resistance of Soils*, Nat. Ctr. for Earthquake Engrg. Res., State Univ. of New York at Buffalo, 89–128.
- Arango, I., 1996, Magnitude scaling factors for soil liquefaction evaluations, *J. Geotech. Engrg., ASCE*, 122(11), 929–936.
- Baise, L. G., Higgins, R. B., and Brankman, C. M., 2006, Liquefaction hazard mapping - Statistical and spatial characterization of susceptible units. *J. Geotech. Geoenviron. Eng.*, 132(6), 705-715.
- Boulanger, R. W., and I.M. Idriss, 2012, Probabilistic standard penetration test-based liquefaction-triggering procedure, *J. Geotech. Geoenviron. Eng.*, 138(10), 1185-1195.
- Broughton, A.T., R.B. Van Arsdale, and J.H. Broughton, 2001, Liquefaction susceptibility mapping in the city of Memphis and Shelby County, Tennessee, *Eng. Geol.* 62, 207-222.
- Bowles, J. E., 1977, *Foundation Analysis and Design*, McGraw-Hill, Inc., New York.
- Brahana, J.V. and Broshears, R.E., 1989, *Hydrogeology and Ground-Water Flow in the Memphis and Fort Pillow Aquifers in the Memphis Area, Tennessee: U.S. Geological Survey Water-Resources Investigations Report 89-4131*, 56 p.

- Brahana, J.V., and Mesko, T.O., 1988, Hydrogeology and preliminary assessment of regional flow in the Upper Cretaceous and adjacent aquifers in the northern Mississippi embayment: U.S. Geological Survey Water-Resources Investigations Report 87-4000, 65 p.
- Broom, M.E., and Lyford, F.P., 1981, Alluvial aquifer of the Cache and St. Francis River basins, northeastern Arkansas: U.S. Geological Survey Open-File Report 81-476, 48 p.
- Cetin, K. O., R.B. Seed, A.D. Kiureghian, K. Tokimatsu, L.F. Harder, R.E. Kayen, and R.E.S. Moss, 2004, Standard penetration test-based probabilistic and deterministic assessment of seismic soil liquefaction potential: *Journal Geotechnical and Geoenvironmental Engineering*, Vol. 130, No. 12, pp. 1314–1340.
- Christopher, B.R. and Schwartz, C., 2006, Geotechnical aspects of pavement reference manual, USDOT pub no. FHWA NHI-05-037, FHA, May, NHI Course no. 132040, 888p.
- Csontos, R.M., 2007, Three dimensional modeling of the Reelfoot rift and New Madrid seismic zone. Ph.D. dissertation, University of Memphis, Memphis, Tennessee, 92 p.
- Cramer, C.H., 2003, Site-specific seismic-hazard analysis that is completely probabilistic, *Bull. Seism. Soc. Am.* 93, 1841-1846.
- Cramer, C.H., 2005, Erratum: Site-specific seismic-hazard analysis that is completely probabilistic, *Bull. Seism. Soc. Am.* 95, 2026.
- Cramer, C.H., 2009, Final Technical Report, a proposal in support of the St. Louis Area Earthquake Hazards Mapping Project: suite of CEUS-specific hard-rock time-histories and seismic hazard model updates, USGS grant 08HQGR0016, February 20, 2009, CERl, 24 pp (available at <http://earthquake.usgs.gov/research/external/reports/08HQGR0016.pdf>).
- Cramer, C.H., 2011, Final Technical Report, a proposal in support of the St. Louis Area Earthquake Hazards Mapping Project: update to methodology and urban hazard map uncertainty analysis, USGS grant 09AP00008, February 14, 2011, CERl, 21 pp (available at <http://earthquake.usgs.gov/research/external/reports/G09AP00008.pdf>).
- Cramer, C.H., and O.S. Boyd, 2014, Why the New Madrid earthquakes are M7–8 and the Charleston earthquake is ~M7, *Bull. Seism. Soc. Am.* **104**, 2884-2903.
- Cramer, C.H., J.S. Gombert, E.S. Scheig, B. A. Waldron, and K. Tucker, 2004, Memphis, Shelby County, Tennessee, seismic hazard maps, U.S. Geological Survey, Open-File Report 04-1294, 41pp.
- Cramer, C.H., J.S. Gombert, E.S. Schweig, B.A. Waldron, and K. Tucker, 2006, First USGS urban seismic hazard maps predict the effects of soils, *Seism. Res. Lett.* 77, 23-29.
- Cramer, C.H., G. Rix, and K. Tucker, 2008, Probabilistic liquefaction hazard maps for Memphis, Tennessee, *Seis. Res. Lett.* 79, 416-423.

- Cramer, C.H., R.B. Van Arsdale, M.S. Dhar, D. Pryne, and J. Paul, 2014, Updating of urban seismic-hazard maps for Memphis and Shelby County, Tennessee: geology and Vs observations, *Seis. Res. Lett.* **85**, 986-996.
- Frankel, A., R. Smalley, and J. Paul, 2012, Significant Motions between GPS Sites in the New Madrid Region: Implications for Seismic Hazard, *Bull. Seism. Soc. Am.* **102**, 479-489.
- Gomberg, J., B. Waldron, E. Schweig, H. Hwang, A. Webbers, R. Van Arsdale, K. Tucker, R. Williams, R. Street, P. Mayne, W. Sphanson, J. Odum, C. Cramer, R. Updike, S. Hutson, and M. Bradley, 2003, Lithology and shear-wave velocity in Memphis, Tennessee, *Bull. Seism. Soc. Am.* **93**, 986-997.
- Graham, D.D., 1982, Effects of urban development on the aquifers of the Memphis area, Tennessee: U.S. Geological Survey Water-Resources Investigations Report 82-4024, 20 p.
- Graham, D.D., and Parks, W.S., 1986, Potential for leakage among principal aquifers in the Memphis area, Tennessee: U.S. Geological Survey Water-Resources Investigations Report 85-4295, 46 p.
- Holzer, T. L., Bennett, M. J., Noce, T. E., Padovani, A. C., and Tinsley III, J. C., 2006, Liquefaction hazard mapping with LPI in the Greater Oakland, California, area. *Earthquake Spectra*, **22**(3), 693-708.
- Hwang, H., M.-C. Chien, and Y.-W. Lin, 1999, Investigation of Soil Conditions in Memphis, Tennessee, USGS Award No. 1434-HQ-98-GR-00002.
- Idriss, I. M., and R.W. Boulanger, 2008, Soil liquefaction during earthquakes. Monograph MNO-12, Earthquake Engineering Research Institute, Oakland, CA.
- Iwasaki, T., Tatsuoka, F., Tokida, K., and Yasuda, S., 1978. A practical method for assessing soil liquefaction potential based on case studies at various sites in Japan, in *Proceedings 2nd International Conference on Microzonation*, pp. 885-896.
- Iwasaki, T., Tokida, K., Tatsuoka, F., Watanabe, S., Yasuda, S., and Sato, H., 1982. Microzonation for soil liquefaction potential using simplified methods, in *Proceedings 3rd International Conference on Microzonation*, pp. 1319-1330.
- Kelson, K.I., Simpson, G.D., Van Arsdale, R.B., Harris, J.B., Haraden, C.C., and Lettis, W.R., 1996, Multiple Late Holocene earthquakes along the Reelfoot fault, central New Madrid seismic zone. *Journal of Geophysical Research*, v. 101, n. B-3, p. 6151-6170.
- Konduru Narsimha, V.K., 2007, Altitudes of ground water levels for 2005 and historic water level change in surficial and Memphis aquifers, Shelby County, Tennessee, Master's Thesis, The University of Memphis, Tennessee.

- Lee, R.C., 2000, A methodology to integrate site response into probabilistic seismic hazard analysis, Site Geotechnical Services, Savannah River Site, report of 3 February 2000.
- Liao, S. S. C., and Whitman, R. V., 1986, Catalogue of liquefaction and non-liquefaction occurrences during earthquakes, Res. Rep., Dept. of Civ. Engrg., Massachusetts Institute of Technology, Cambridge, Mass.
- Luna, R., and Frost, J., 1998, Spatial Liquefaction Analysis System, J. Comput. Civ. Eng., 12(1), 48-56.
- Ng K. W., Chang, T-S., and Hwang H-H. M., 1989, Subsurface Conditionns of Memphis and Shelby County, Technical Report NCEER-89-0021.
- NWIS, 2015, <http://nwis.waterdata.usgs.gov/tn/nwis/gwlevels>, last accessed on September 2015.
- Park, W.S., 1990, Hydrogeology and preliminary assessment of the potential for contamination of the Memphis aquifer in the Memphis area, Tennessee. Water-Resources Investigations Report 90-4092. Available at <http://pubs.er.usgs.gov/publication/wri904092>
- Petersen, M.D., M.P. Moschetti, P.M. Powers, C.S. Mueller, K.H. Haller, A.D. Frankel, Y. Zeng, S. Rezaeian, S.C. Harmsen, O.S. Boyd, N. Field, R. Chen, K.S. Rukstales, N. Luco, R.L. Wheeler, R.A. Williams, and A.H. Olsen, 2014, Documentation for the 2014 update of the United States national seismic hazard maps, USGS Open-file Report 2014-1091, 255 p.
- Plebuch, R.O., 1961, Fresh-water aquifers of Crittenden County, Arkansas: Arkansas Geology and Conservation Commission Water Resources Circular no. 8, 65 p.
- Reiter, L., 1990, Earthquake Hazard Analysis: Issues and Insights, Columbia University Press, New York.
- Rix, G. J. and S. Romero-Hudock, 2006, Liquefaction potential mapping in Memphis and Shelby County, Tennessee, unpublished Rept. To the U.S. Geol. Surv., Denver, Colorado, 27 pp: available at http://earthquake.usgs.gov/hazards/products/urban/memphis/Memphis_LPI.pdf, last accessed September 2015.
- Rix, G. J., 2001, Liquefaction Susceptibility Mapping in Memphis/Shelby County, TN, USGS Award No. 01-HQ-AG-0019
- Robertson, P. K., and Wride, C. E., 1998, Evaluating cyclic liquefaction potential using the cone penetration test, Canadian Geotechnical Journal, 35 442-459.
- Romero S., and G.J. Rix, 2001, Regional variations in near surface shear wave velocity in the Greater Memphis area, Eng. Geol. 62, 137-158.
- Seed, H.B. and Idriss, I.M., 1971. Simplified procedure for evaluating soil liquefaction potential,

Journal of the Soil Mechanics and Foundations Division 97, 1249-1273.

Seed, H. B., and Idriss, I. M., 1982, Ground motions and soil liquefaction during earthquakes, Earthquake Engineering Research Institute Monograph, Oakland, Calif.

Stevens, K.C., 2007, A structural interpretation of near-surface borehole data in Shelby County, Tennessee, Masters Thesis, University of Memphis, 60 pp.

Toprak, S., and Holzer, T. L., 2003, Liquefaction potential index: Field assessment, J.Geotech.Geoenviron.Eng., 129(4), 315-322.

Tuttle, M. P., E. S., Schweig, J. D. Sims, R. H. Lafferty, L. W. Wolf, and M. L. Haynes, 2002, The earthquake potential of the New Madrid seismic zone, Bull. Seism. Soc. Am., 92, 2080–2089.

Tuttle, M.P., H. Al-Shukri, and H. Mahdi, 2006, Very large earthquakes centered southwest of the New Madrid seismic zone 5,000-7,000 years ago, Seis. Res. Ltrrs. 77, 755-770.

Wells, F.G., 1933, A preliminary report on the artesian water supply of Memphis, Tennessee: U.S. Geological Survey Water-Supply Paper 638-A, 34 p.

Youd, T. L., and Idriss, I. M., 2001, Liquefaction Resistance of Soils: Summary Report from the 1996 NCEER and 1998 NCEER/NSF Workshops on Evaluation of Liquefaction Resistance of Soils, Journal of Geotechnical and Geoenvironmental Engineering, 127(4), 297-313.

Youd, T.L., Idriss, I.M., Andrus, R.D., Arango, I., Castro, G., Christian, J.T., Dobry, R., Finn, W.D.L., Harder, L.F. Jr., Hynes, M.E., Ishihara, K., Koester, J.P., Liao, S.S.C., Marcuson, W.F. III, Martin, G.R., Mitchell, J.K., Moriwaki, Y., Power, M.S., Robertson, P.K., Seed, R.B., and Stokoe, K.H. II, 2001, Liquefaction resistance of soils: Summary report from the 1996 NCEER 14 and 1998 NCEER/NSF workshop on evaluation of liquefaction resistance of soils, Journal of Geotechnical and Geoenvironmental Engineering 127, 817-833.

Youd, T. L., and Noble, S. K., 1997a, Magnitude scaling factors, Proc., NCEER Workshop on Evaluation of Liquefaction Resistance of Soils, Nat. Ctr. for Earthquake Engrg. Res., State Univ. of New York at Buffalo, 149–165.

Youd, T. L., and Noble, S. K., 1997b, Liquefaction criteria based on statistical and probabilistic analyses, Proc., NCEER Workshop on Evaluation of Liquefaction Resistance of Soils, Nat. Ctr. for Earthquake Engrg. Res., State Univ. of New York at Buffalo, 201–215.

Publications from this Research

No publications have resulted from this research as of this date. Future papers based on this work will be provided, as required, when publication occurs.

Appendix A – Workshop Agenda



MEMPHIS AREA EARTHQUAKE HAZARDS MAPPING PROJECT WORKSHOP
JULY 28, 2015
Bass Pro Pyramid, Big Cypress Hotel Conference Area
8:30 AM – 3:00 PM

Sponsors: West Tennessee Seismic Safety Commission, U.S. Geological Survey, Mid-South Association of Contingency Planners, State Farm Insurance, and the Center for Earthquake Research and Information at the University of Memphis.

Please park on the South side of the Pyramid and go to the Big Cypress Hotel elevators at the South entrance and up to the third floor. Follow the signs to the meeting room.

Workshop Agenda

8:30 Registration and Coffee

9:00 Understanding Urban Earthquake Hazard Maps:

Welcome and Introductions – Gary Patterson [CERI] and Elly Jones [State Farm/WTNSSC] (10 min)

How Have Urban Hazard Maps Helped Communities – Rob Williams [USGS] (15 min)

Project Overview and New Memphis Maps – Chris Cramer [CERI] (30 min)

Geotechnical Update in Hazard Maps – David Arellano [U Memphis] (30 min)

Ground Water Levels in Shelby Co. – Scott Schoefernacker [GWI] (15 min)

10:40 Break

11:00 Why Liquefaction is Important:

Christchurch, NZ: Liquefaction Lessons for Memphis – Russell Green [Virginia Tech] (30 min)

Earthquake Hazard Mitigation in Memphis – Ashref Elsayed [Geotechnology] (30 min)

12:00 Lunch – Salad or Sandwich

12:20 Lunch Speaker: David Johnston – Christchurch and Memphis [GNS Science New Zealand] (60 min)

1:30 Using the Maps and Mitigation Efforts – Panel with examples and discussion:

Utilities – Callen Hays, Jay Stressel [MLGW] (10 min)

Emergency Managers – Brent Phillips [TEMA] (10 min)

Business Continuity – Ronnie Smith [MSACP/First Horizon] (10 min)

Urban Planning, Government – Philip Boruszewski [USCG] (10 min)

2:30 Plenary Discussion – Who Needs to Know About and Use Hazard Maps?

At the Start, What We Heard About User Needs – Chris Cramer [CERI] (5 min)

Discussion on Where We Go From Here and Additional Needs – All

3:00 Closing remarks – Chris Cramer [CERI] (5 min)



Appendix B - Attendees

MAEHMP July 28, 2015 Workshop Registration

Name	Email	Organization
Ambroise-Hurst, Shayla	Shayla.Ambroise@ipaper.com	International Paper
Anderson, Ashton	Ashton.Anderson@shelbycou	Shelby Co Health Dept.
Arellano, David	darellan@memphis.edu	CivEng, U of M
Ausbrooks, Scott	laura.hinze@arkansas.gov	AR GS Contact Email
Avanzi, Michael	savanzi@mlgw.org	MLGW
Bailley, Jeana	Jeana.Bailley@redcross.org	Red Cross
Barr, Brian	Brian.Barr@ipaper.com	International Paper
Bass, Eddie	Eddie.Bass@memphistn.gov	MPD
Bennet, Royal	Royal.Bennett@servicemaste	MSACP, ServiceMaster
Benson, Linda	Linda.Benson@memphistn.g	Fire Svcs OEM
Bledsoe, Janet	jmbledsoe@fedex.com	FedEx
Bone, Cheryl	grandmapiq@rittermail.com	Hope for the Midsouth
Boruszewski, Philip	Philip.H.Boruszewski@uscg.n	US Coast Guard
Bowker, Rick	Rbowker@mlgw.org	MLGW
Boyd, G. Herman	docboy01@yahoo.com	
Boyd, Oliver	olboyd@usgs.gov	USGS
Brignole, Pat	Pat_Brignole@tnwd.uscourts	WDTN US Courts
Brooks, Albert	abrooks@mlgw.org	MLGW
Brown, Kenneth	Kenneth.Brown@memphistn	Fire Svcs OEM
Bucy, John	John.Bucy@nwtdd.org	WTNSSC
Bullock, Bill	Bbullock@mlgw.org	MLGW
Caldwell, Philip	phil.caldwell@nonstructural.c	Schneider Electric
Cameron, Mike	mcameron@mlgw.org	MLGW
Carson, Gale	galecarson@mlgw.org	MLGW
Chapple, Carol	carol5340@att.net	Fire Svcs OEM
Cheeks, Leimome	ljcheeks@fedex.com	FedEx
Clark, Quinton	qclark@mlgw.org	MLGW
Clarkson, Kevin	Sandy.Stettler@cbrememphi	CBRE Memphis
Cole, Deborah	dccole@fedex.com	FedEx
Cox, Randy	randycox@memphis.edu	DES, U of M
Craig, Alan	kradams@fedex.com	FedEx
Cramer, Chris	ccramer@memphis.edu	CERI, U of M
Crenshaw, Scott	ecrenshaw@fedex.com	FedEx
Darby, Monica	mdarby@mlgw.org	MLGW
David, johnston	laura.hinze@arkansas.gov	AR GS
Davis, Alexander	Alexander.Davis@redcross.or	Red Cross
DeBerry, Clifford	cdeberry@mlgw.org	MLGW
Dhar, Mahesh	msdhar@memphis.edu	CERI, U of M
Dill, James	james.s.dill@navy.mil	EMP Manager, NSAMS
Duncan, Doug	dmduncan@mlgw.org	MLGW
Dyson, Alfred	a_dyson@msn.com	Dyson Engineering
Edwards, David	dedwards@mlgw.org	MLGW
Ellis, Wayne	wellis@mlgw.org	MLGW
Elsayed, Ashraf	A_Elsayed@geotechnology.cc	Geotechnology
Embry, Jeff	jembry@mlgw.org	MLGW
Fleischer, Jeanette	Jeanette.Fleischer@cbremerr	CBRE Memphis
Foreman, Justin	Justin_Foreman@tnwb.uscou	WDTN US Courts

Fortner, Heather	heather.fortner@shelbycount	Shelby Co Health Dept.
Freed, William	William.Freed@memphistn.g	MPD
Gould, Tom	Tom_Gould@tnwd.uscourts.g	WDTN US Courts
Graves, Gary	g,graves@millingtontn.gov	WTNSSC
Graves, Lauren	Lauren.L.Graves@usace.arm	USACE
Green, Russell	rugreen@vt.edu	VaTech
Harris, Felicia	Felicia.Harris@memphistn.go	Planning and Development, C
Harvill, James	James.Harvill@memphistn.gc	MFD
Haston, Angie	phyllis.basinger.ckbh@statef	State Farm
Hawk, Charles	charles.hawk@fedex.com	FedEx
Hays, Callen	CHays@mlgw.org	MLGW
Horton, Steve	shorton@memphis.edu	WTNSSC, CERI
Howe, Rick	rwhowe@earthlink.net	R.W. Howe Assoc.
Hughes, Michael	michael.hughes@cbremempl	CBRE Memphis
Hunt, Phyllis	PHunt@mlgw.org	MLGW
Jackson, Wayne	wjjackson@mlgw.org	MLGW
Jennings, Marcus	marcus.jennings@shelbycour	Shelby Co Health Dept.
Johnston, David	David.Johnston@gns.cri.nz	GNS NZ
Jones, Elly	elly.jones.c46g@statefarm.cc	WTNSSC, State Farm
Jones, Eugene	Eugene.Jones@shelbycounty	Shelby Co Office of Preparedr
Kost, Scott	john.kost@fedex.com	FedEx
Kowalski, Elizabeth		Hope for the Midsouth
Kurlick, Tom	Tom.Kurlick@BMHCC.org	Baptist Health Care
Lambie, Emily	emily_lambie@windowslive.c	GNS NZ
Lane, Dale	Dale.Lane@shelbycountytn.g	Shelby Co Office of Preparedr
Laster, Eddie	Eddie.Laster@usdoj.gov	USMS, Memphis
Lawrence, Tom	tomlawrence@bellsouth.net	
Lewis, Nicholas	Nicolas.Lewis@BMHCC.org	Baptist Memphis Hospitals
Livingston, Mark	MELivingston@firsthorizon.cc	First Horizon
Lock, Dale	Dale.Lock@memphistn.gov	MFD
Logan, Lt. Jim		Fire Svcs OEM
Lombardo, Ray	rlombardo@mlgw.org	MLGW
Mabon, Vernon	mabonvm@aol.com	
Mabry, Parker	parker.mabry@memphistn.gc	SAIC City of Memphis
Mackenzie, Owen	mowen@meri.org	MERI
Mansel, Jan	jan@ppmrealtymemphis.com	PPM Realty
Martin, Bobby	bmartin@fayettetn.us	Fayette Co
Mashburn, Phillip	phillipm@ctsi-qlobal.com	CTSI Global
McCaig, William	wmccaig@mlgw.org	MLGW
McElyea, Philip		UHSINC
McGuire, Mark	Mark.McGuire@memphistn.g	Memphis
Montgomery, Christi	christi.montgomery@navy.m	US Navy
Moore, Barry	barrywmoorerehs@gmail.com	WTNSSC
Moss, Tammy	tmoss@keithcollinsco.com	Keith S. Collins Co
Mosteller, Jon	jmosteller@mlgw.org	MLGW
Nash, Andy	andyn@tnwd.uscourts.gov	WDTN US Courts
Nunley, David	dnunley@sco.edu	Southern College of Optomet
Oates, Junius	Junius.K.Oates@uscg.mil	US Coast Guard
Orchiston, Caroline		GNS NZ

Palmisano, Robert	Rpalmisano@bellsouh.net	The Palmisano Group
Parker, Greg	Greg.Parker@shelbycountytn.gov	Shelby Co Health Dept.
Parker, Irene	ilparker@fedex.com	FedEx
Parker, Kevin	Kevin.Parker@uhsinc.com	UHSINC
Pasley, Kim	kpasley@mlgw.org	MLGW
Patterson, Gary	glpttrsn@memphis.edu	CERI, U of M
Perry, Sue	scperry@usgs.gov	USGS
Pettis, Pamela	ppetis@mlgw.org	MLGW
Pezeshk, Shahram	spezeshk@memphis.edu	CivEng, U of M
Phillips, Brent	BPhillips@tnema.org	TEMA
Pilant, Landon	landon.pilant@fedex.com	FedEx
Powers, Craig	cpowers@mlgw.org	MLGW
Robertson, Blake	Blake.Robertson@lebonheur.us	Le Bonheur
Rousseau, Kelley	Kelley_Rousseau@tnwb.usco.us	USBC, WDTN
Rudolph, Jordan	jrudolph@mlgw.org	MLGW
Rutledge, Chris	crutledge@mlgw.org	MLGW
Sansone, Steven	Steven.A.Sansone@usace.army.mil	USACE
Schoefernacker, Scott	sschfnrc@memphis.edu	GWI, U of M
Silbee, Laura	Laura.Silbee@memphistn.gov	MFD ?
Smith, Bill	Bill.Smith@shelbycountytn.gov	Shelby Co Health Dept.
Smith, Ronald	ronald.smith@fedex.com	PR Director, MSACP
Smith, Ronnie	rgsmith@firsthorizon.com	First Horizon
Sowell, Donnie	dsowell@psgi.net	ProTech Systems Group, Inc.
Stewart, Charles	charles.stewart@memphistn.gov	Fire Svcs OEM
Stressel, Jay	jstressel@mlgw.org	MLGW
Strongosky, Neil	nstrongosky@mlgw.org	MLGW
Todd, Sharon	stodd@mlgw.org	MLGW
Townsend, Brenda	btownsend@mlgw.org	MLGW
Trammell, Renee	rtrammell@regionalonehealth.com	Regional One Health
Tutor, Rachel	rtwade@firsthorizon.com	First Horizon
Valencius, Conevery	Conevery.Valencius@umb.edu	Umass Boston
VanSickel, Gregory	GVanSickel@mlgw.org	MLGW
Vaughn, Lassell	lvaughn@mlgw.org	MLGW
Wery, Rick	rwery@mlgw.org	MLGW
Wherry, Tracy	tracy_wherry@tnwd.uscourts.gov	WDTN US Courts
Williams, Keisha	KWilliams@mlgw.org	MLGW
Williams, Rob	rawilliams@usgs.gov	USGS
Winford, William "Tom"	wwinford@mlgw.org	MLGW
Wood, Clinton	cmwood@uark.edu	U of AR, Fayetteville
Woodall, Gary	gary.woodall@noaa.gov	Natl Weather Service Memphi
Zeng, Jason	jian.Zeng@fedex.com	FedEx